Electroweak baryogenesis in aligned two Higgs doublet model

Yushi Mura (Osaka U. PhD student)

Kazuki Enomoto (U. of Tokyo.) and Shinya Kanemura (Osaka U.)

2022/8/31 Workshop on Multi Higgs Models 2022 in Lisboa

Based on

K. Enomoto, S. Kanemura, and Y.M, JHEP 01 (2022) 104, arXiv: 2111.13079 [hep-ph]

and

K. Enomoto, S. Kanemura, and Y.M, arXiv: 2207.00060 [hep-ph] (to appear in JHEP)

Dr. Wani, OU mascot

Introduction

Standard Model cannot explain the Baryon Asymmetry of the Universe.

Observed baryon asymmetry from Big Bang Nucleosynthesis,

$$\eta_B^{obs} = \frac{n_B}{n_\gamma} = 5.8 - 6.5 \times 10^{-10}$$ PDG (2020)

This asymmetry is generated at the early Universe ⇨ Baryogenesis

For Baryogenesis,

Sakharov's Conditions Sakharov, Pisma Zh. Eksp. Teor. Fiz. 5 (1967)

① Baryon number violation
② C and CP violation
③ Out of thermal equilibrium

must be satisfied.

Some possibilities

- Affleck-Dine mechanism — Affleck and Dine, Nucl. Phys. B 249 (1985)
- Electroweak baryogenesis — Kuzmin, Rubakov and Shaposhnikov, Phys Lett. B 155 (1985)
- Leptogenesis — Fukugita and Yanagida, Phys. Lett. B 174 (1986)

etc.

Electroweak baryogenesis

Sakharov's Conditioins
① Baryon number violation
② C and CP violation
③ Out of thermal equilibrium

Electroweak Baryogenesis (EWBG)

① Sphaleron process
② C violation in chiral theory,
CP violation in Higgs sector
③ Strongly first order electroweak phase transition

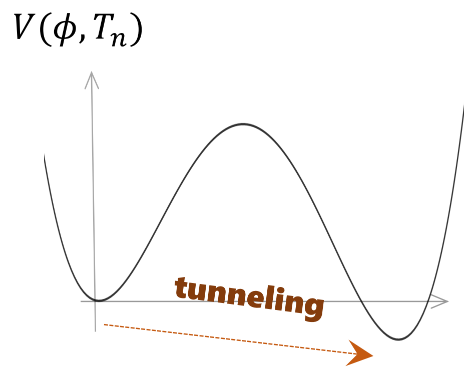

After the first order phase transition,

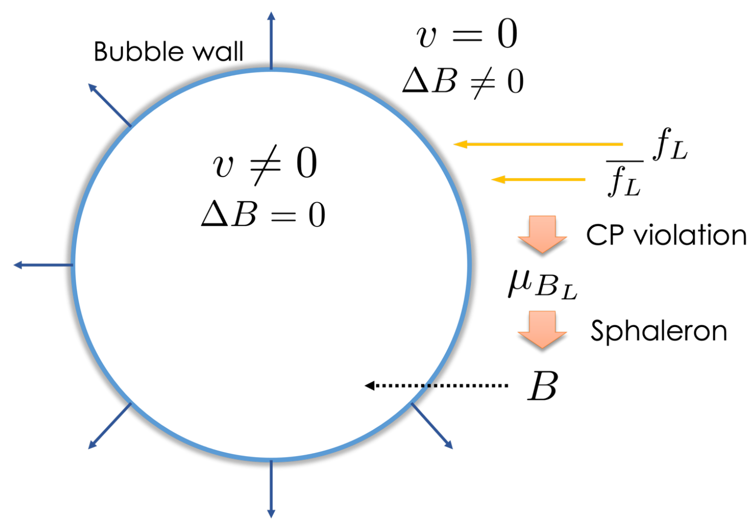

baryon number is created around the wall.

To decouple sphaleron process

$$\Gamma_{sph}^{brk}(T_n) < H(T_n) \Longrightarrow \frac{v_n}{T_n} \gtrsim 1$$

→ "Strongly" first order PT

Recent

Huet and Sather, Phys. Rev. D 51 (1995)
Kajantie *et al.* Phys. Rev. Lett. 77 (1996)

However, EWBG in the SM is not realized.

- Insufficient CPV
- Not occur first order EWPT

⇨ **Extended Higgs sector is needed !**

⇨ **EWBG can be tested by the future Higgs precision experiments !**

Ex) Two Higgs Doublet Model

Fromme, Huber and Seniuchi, JHEP 11 (2006); Cline, Kainulainen and Trott, JHEP 11 (2011); Dorsch et al. JCAP 05 (2017); and more

After the discovery of Higgs boson in 2012,

- **LHC exp.** SM like Higgs couplings

Aad *et al.* [ATLAS] Phys. Rev. D 101 (2020); Sirunyan *et al.* [CMS] Eur. Phys. J. C 79 (2019)

- **Electric Dipole Moment exp.** Severe constraints on additional CPV

Andreev *et al.* [ACME] Nature 562 (2018)

In such situation, Kanemura, Kubota and Yagyu, JHEP 08 (2020)

- SM like Higgs boson
- Destructive interference between CPV phases

Todays talk about..

We show some benchmarks can explain BAU under current data in THDM.
Also discuss some phenomenological consequences.

K. Enomoto, S. Kanemura, and Y.M, JHEP 01 (2022) 104
K. Enomoto, S. Kanemura, and Y.M, 2207.00060 [hep-ph] (to appear in JHEP)

Aligned Two Higgs Doublet Model

The most general potential

$$\Phi_1 = \begin{pmatrix} G^+ \\ \frac{1}{\sqrt{2}}(v + h_1 + iG^0) \end{pmatrix}, \qquad \Phi_2 = \begin{pmatrix} H^+ \\ \frac{1}{\sqrt{2}}(h_2 + ih_3) \end{pmatrix}$$

$$V = -\mu_1{}^2(\Phi_1{}^\dagger\Phi_1) - \mu_2{}^2(\Phi_2{}^\dagger\Phi_2) - \left(\mu_3{}^2(\Phi_1{}^\dagger\Phi_2) + h.c.\right)$$

Higgs basis Davidson and Haber, Phys. Rev. D 72 (2005)

$$+ \frac{1}{2}\lambda_1(\Phi_1{}^\dagger\Phi_1)^2 + \frac{1}{2}\lambda_2(\Phi_2{}^\dagger\Phi_2)^2 + \lambda_3(\Phi_1{}^\dagger\Phi_1)(\Phi_2{}^\dagger\Phi_2) + \lambda_4(\Phi_2{}^\dagger\Phi_1)(\Phi_1{}^\dagger\Phi_2)$$

$$+ \left\{\left(\frac{1}{2}\lambda_5\Phi_1{}^\dagger\Phi_2 + \lambda_6\Phi_1{}^\dagger\Phi_1 + \lambda_7\Phi_2{}^\dagger\Phi_2\right)\Phi_1{}^\dagger\Phi_2 + h.c.\right\}, \quad (\mu_3, \lambda_5, \lambda_6, \lambda_7 \in \mathbb{C})$$

Mass spectrum

Charged scalar $\quad m_{H^\pm}^2 = M^2 + \frac{1}{2}\lambda_3 v^2 \qquad M^2 \equiv -\mu_2^2$

Neutral scalar

$$\mathcal{M}^2 = v^2 \begin{pmatrix} \lambda_1 & \boxed{\mathrm{Re}\lambda_6} & \boxed{-\mathrm{Im}\lambda_6} \\ \boxed{\mathrm{Re}\lambda_6} & \frac{M^2}{v^2} + \frac{\lambda_3+\lambda_4+\mathrm{Re}\lambda_5}{2} & \cancel{-\frac{1}{2}\mathrm{Im}\lambda_5} \\ \boxed{-\mathrm{Im}\lambda_6} & \cancel{-\frac{1}{2}\mathrm{Im}\lambda_5} & \frac{M^2}{v^2} + \frac{\lambda_3+\lambda_4-\mathrm{Re}\lambda_5}{2} \end{pmatrix}$$

By phase redefinition

Experimental fact "mixing angle among neutral scalars is small"

For simplicity, we set $\lambda_6 = 0$ (Higher loop corrections are non-zero)

$$= \begin{pmatrix} m_h^2 & 0 & 0 \\ 0 & m_{H_2}^2 & 0 \\ 0 & 0 & m_{H_3}^2 \end{pmatrix}$$

Coupling consts. coincide with SM ones

Higgs alignment

Finally, only the CP phase $\arg[\lambda_7] \equiv \theta_7$ remains.

Aligned Two Higgs Doublet Model

The most general Yukawa interaction

$$-\mathcal{L}_y = \sum_{k=1}^{2} \left(\overline{Q}'_L (y_u^k)^\dagger \tilde{\Phi}_k u'_R + \overline{Q}'_L y_d^k \Phi_k d'_R + \overline{L}'_L y_e^k \Phi_k e'_R + h.c. \right)$$

Experimental fact "Flavor Changing Neutral Current must be suppressed"

We assume $y_f^2 = \zeta_f y_f^1 \quad (f = u, d, e)$ Yukawa alignment

Pich and Tuzon, Phys. Rev. D 80 (2009)

$\zeta_u, \zeta_d, \zeta_e \in \mathbb{C}$

$$\mathcal{L}_y = -\overline{Q}_L \frac{\sqrt{2}M_u}{v} \left(\tilde{\Phi}_1 + \zeta_u^* \tilde{\Phi}_2 \right) u_R - \overline{Q}_L \frac{\sqrt{2}M_d}{v} \left(\Phi_1 + \zeta_d \Phi_2 \right) d_R - \overline{L}_L \frac{\sqrt{2}M_e}{v} \left(\Phi_1 + \zeta_e \Phi_2 \right) e_R + h.c.$$

Summary of CP phases in the model

Potential $\arg[\lambda_7] \equiv \theta_7$

Yukawa $\arg[\zeta_u] \equiv \theta_u$, $\arg[\zeta_d] \equiv \theta_d$, $\arg[\zeta_e] \equiv \theta_e$

Constraints on the model

Severe electron EDM bound

$|d_e| < 1.1\times 10^{-29} e$ cm

Andreev *et al.* [ACME] Nature 562 (2018)

Avoiding EDM bound with destructive interference

$d_e \simeq$

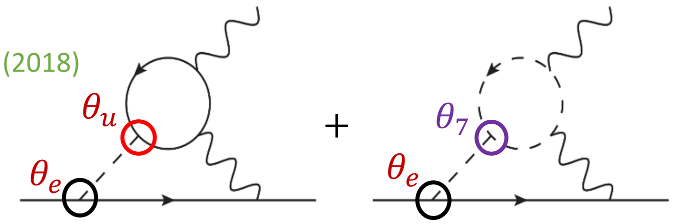

(a) Fermion-loop. (b) Higgs boson-loop.

Kanemura, Kubota and Yagyu, JHEP 08 (2020)

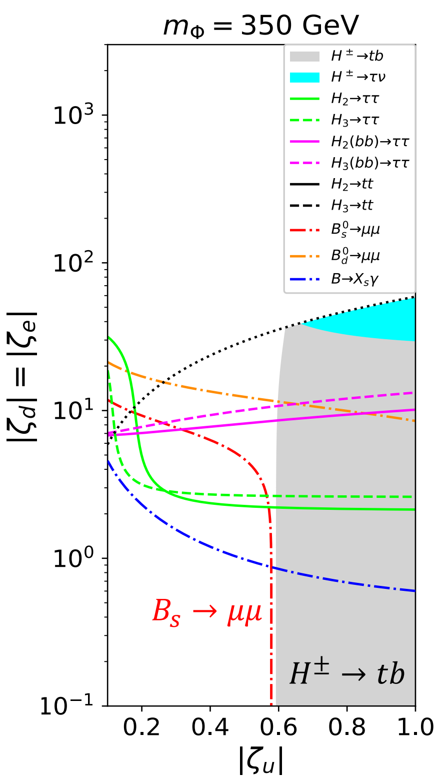

Direct search exp.

$H_{2,3} \to \tau\tau$ Aad *et al.* [ATLAS] Phys. Rev. Lett. 125 (2020)

$H_{2,3}(bb) \to \tau\tau$

$H_{2,3} \to tt$ Aaboud *et al.* [ATLAS] Eur. Phys. J. C 78 (2018); Sirunyan *et al.* [CMS] JHEP 04 (2020)

$H^\pm \to tb$ Aad *et al.* [ATLAS] JHEP 06 (2021)

$H^\pm \to \tau\nu$ Sirunyan *et al.* [CMS] JHEP 07 (2019)

Flavor exp.

$B_d \to \mu\mu$ Amhis *et al.* [HFLAV] Eur. Phys. J. C 81 (2021); Haller *et al.* Eur. Phys. J. C 78 (2018);

$B_s \to \mu\mu$ Aaboud *et al.* [ATLAS] JHEP 04 (2019); Sirunyan *et al.* [CMS] JHEP 04 (2020);

$B \to X_s\gamma$ Aaij. *et al.* [LHCb] Phys. Rev. D 105 (2022)

ζ_u is important for BAU and we found $|\zeta_u| \lesssim 0.6$

We also considered,

$m_\Phi \equiv m_{H_2} = m_{H_3} = m_{H^\pm}$

neutron EDM, STU parameters, perturbative unitarity, vacuum stability

Baryogenesis

Inputs

$M = 30\,\mathrm{GeV},\ \lambda_2 = 0.1,\ |\lambda_7| = 0.8,\ \theta_7 = -0.9,$

$|\zeta_u| = |\zeta_d| = |\zeta_e| = 0.18,\ \theta_u = -2.7,\ \delta_d = 0,\ \delta_e = -0.04.$

relate to.. BAU / eEDM / both

Baryon asymmetry in the relativistic bubble wall velocity Cline and Kainulainen, Phys. Rev. D 101 (2020)

The observed BAU (pink) $\eta_{obs}^{\mathrm{BBN}} \equiv \frac{n_B}{s} = 8.2\text{–}9.2 \times 10^{-11}$

Electron EDM (blue dotted)

We set two benchmarks : BP1: strongly PT; BP2: weakly PT

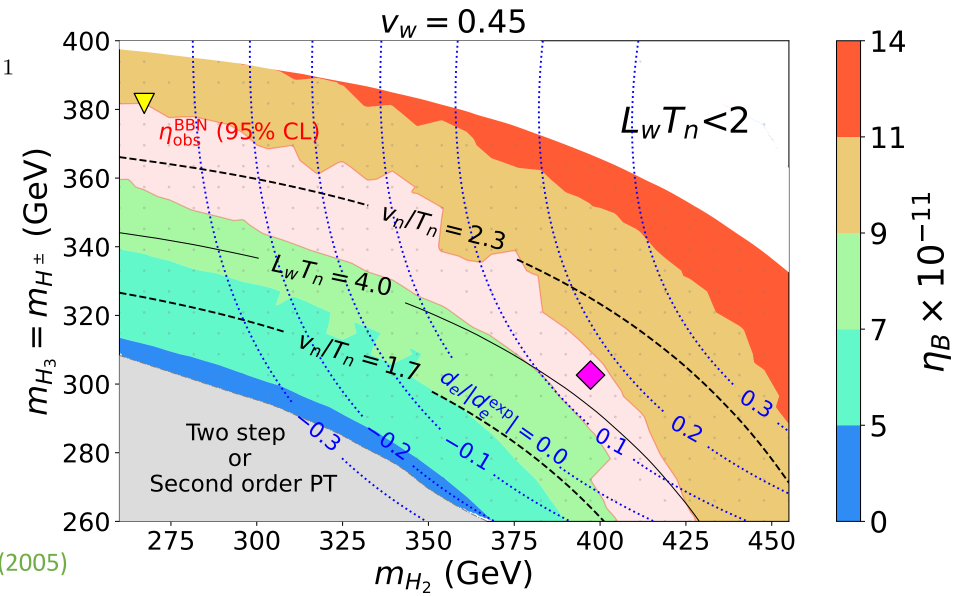

First order PT and non-decoupling effect

Deviation of triple Higgs coupling

Kanemura, Okada and Senaha, Phys. Lett. B 606 (2005)

$(\Delta R \equiv \delta\lambda_{hhh}/\lambda_{hhh}^{SM})$

Strongly PT (BP1) $\Delta R = 61\%$

Weakly PT (BP2) $\Delta R = 44\%$ $\Rightarrow$ **Detectable in future colliders**

Ex) HL-LHC : 50%
ILC (500 GeV) : 27%
ILC (1 TeV) : 10%

Capeda *et al.* CERN Yellow Rep. Monogr. 7 (2019); Fujii *et al.* [1506.05992]; Bambade *et al.* [1903.01629]

Higgs to di-photon decay

Ellis, Gaillard and Nanopoulos, Nucl. Phys. B 106 (1976); Shifman *et al.* Sov. J. Nucl. Phys. 30 (1979); and more works

In each BP,

$$\sigma Br(H_1 \to \gamma\gamma) = 104 \pm 5\ \mathrm{fb}$$

SM: $\sigma Br(H_1 \to \gamma\gamma)_{SM} = 116 \pm 5$ fb

Observed: $\sigma Br(H_1 \to \gamma\gamma)_{obs} = 127 \pm 10$ fb

ATLAS-CONF-2020-026

At HL-LHC, uncertainty ~3%

Capeda *et al.* CERN Yellow Rep. Monogr. 7 (2019)

Gravitational waves

Gravitational wave spectra

Grojean and Servant, Phys. Rev. D 75 (2007);
Kakizaki, Kanemura and Matsui, Phys. Rev. D 92 (2015); and more

Sensitivity curves Hashino *et al.* Phys. Rev. D 99 (2019)

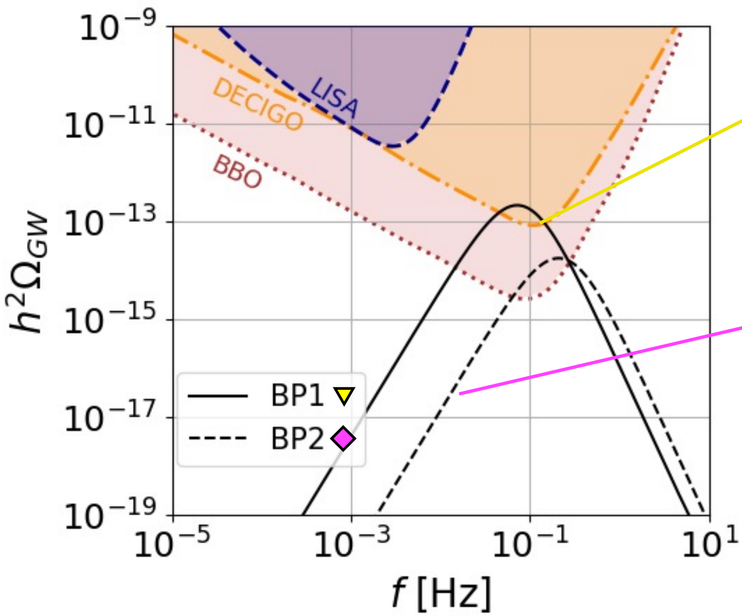

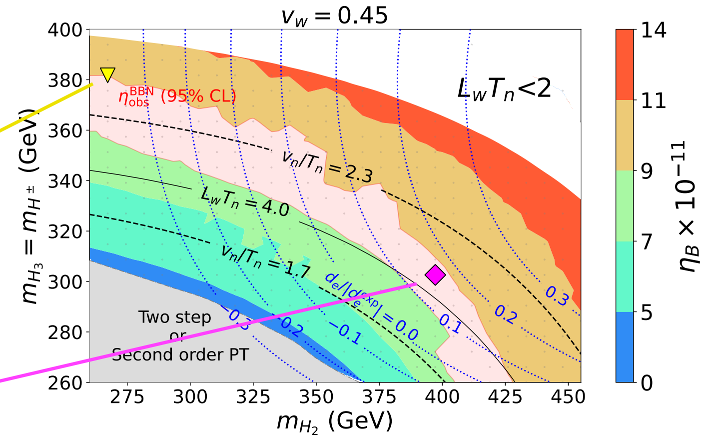

▽ BP1: strongly PT

◆ BP2: weakly PT

Strong PT is needed for predictable GWs.

BP1 and BP2 can also be tested by GW observation.

Phenomenology of CP violation

various EDM, flavor and collider exp. (see back up)

Summary

◆ SM cannot explain the Baryon asymmetry of the universe

EWBG as a solution of BAU is Higgs physics thus it is testable.

◆ Aligned Two Higgs Doublet Model

- SM like 125 GeV Higgs boson
- We showed the BAU can be explained under current data.
- Additionally, some of BPs can be tested using GW signal.

◆ Phenomenology

- Higgs triple coupling ⇒ HL-LHC, ILC (500GeV, 1TeV)
- Higgs to di-photon ⇒ HL-LHC
- Gravitational waves ⇒ LISA, DECIGO, BBO
- Additional CPV ⇒ EDM, Flavor, ILC (see back up)

Back up

Predictions of CP violation

CPV in the future flavor experiments

Benzke *et al.* Phys. Rev. Lett. 106 (2011);
Watanuki *et al.* [Belle] Phys. Rev. D 99 (2019); and more

$$\Delta A_{CP} = A_{CP}(B^+ \to X_s^+ \gamma) - A_{CP}(B^0 \to X_s^0 \gamma)$$

$$A_{CP}(X \to Y) \equiv \frac{\Gamma(\bar{X} \to \bar{Y}) - \Gamma(X \to Y)}{\Gamma(\bar{X} \to \bar{Y}) + \Gamma(X \to Y)}$$

Solid : current excluded
Dashed : future excluded (Belle Ⅱ)

ζ_d can be constrained from the future flavor exp.

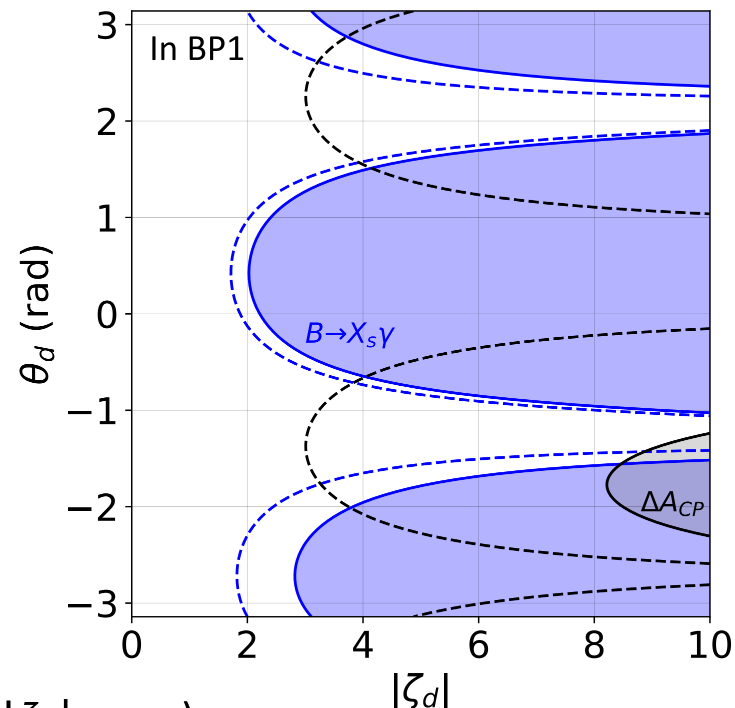

CPV in the decays of the neutral scalar bosons ($|\zeta_d| \ll |\zeta_e|$ case)

Azimuth angle dependence in $H_{2,3} \to \tau^+\tau^- \to X^+\bar{\nu}X^-\nu$

Kanemura, Kubota and Yagyu, JHEP 04 (2021)

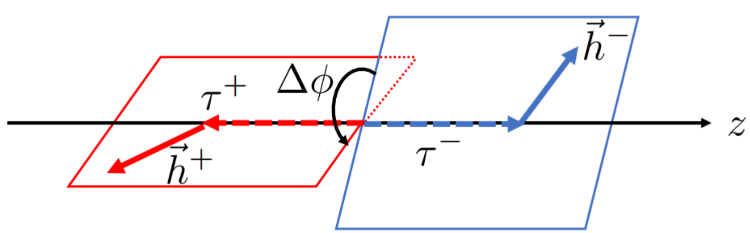

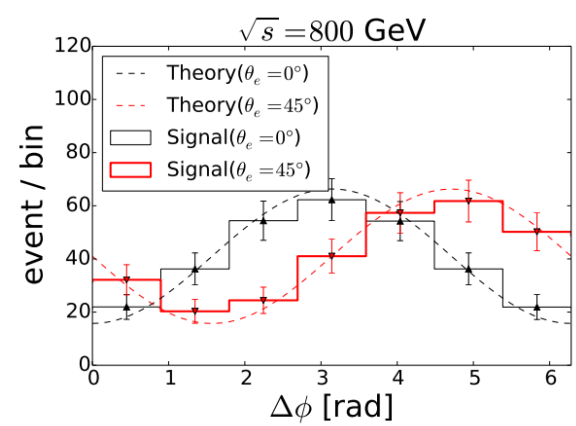

Detectability of the phase of ζ_e in ILC

Neutron EDM

Experimental bound: $|d_n| < 1.8{\times}10^{-26} e$ cm Abel *et al.* [nEDM] Phys. Rev. Lett. 124 (2020)

ζ_d is restricted from neutron EDM.
The leading graph is chromo Barr-Zee type of down quark.

$d_n \supset$ 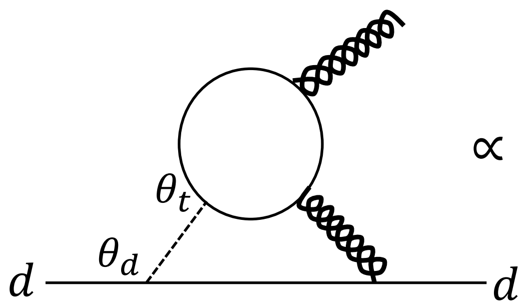

$\propto |\zeta_u||\zeta_d|\sin(\theta_u - \theta_d)$

In BP1

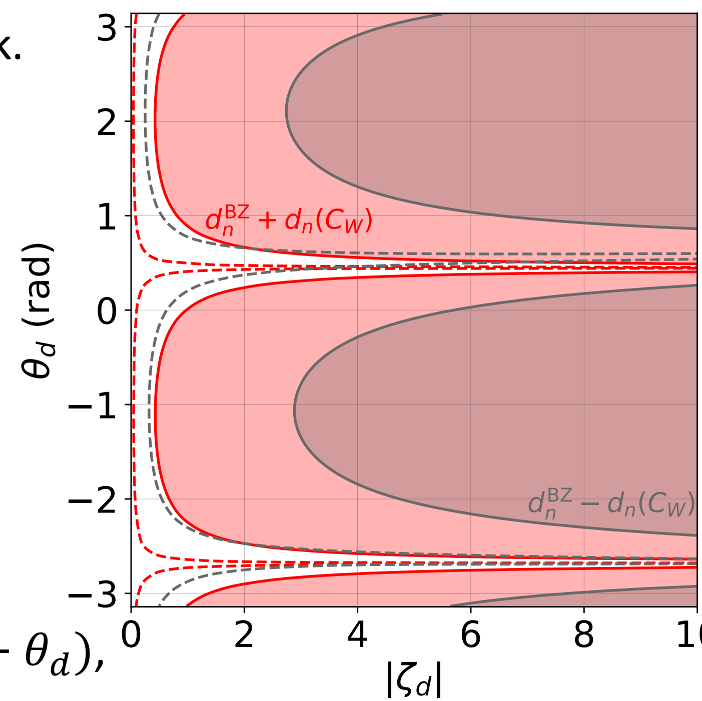

Also, from Weinberg operator $d_n(C_W) \propto |\zeta_u||\zeta_d|\sin(\theta_u - \theta_d)$,
but the sign of $d_n(C_W)$ is not determined.

Solid: current
Dashed: expected

Red: $d_n^{BZ} + d_n(C_W)$ case
Gray: $d_n^{BZ} - d_n(C_W)$ case

Velocity dep. of baryon density

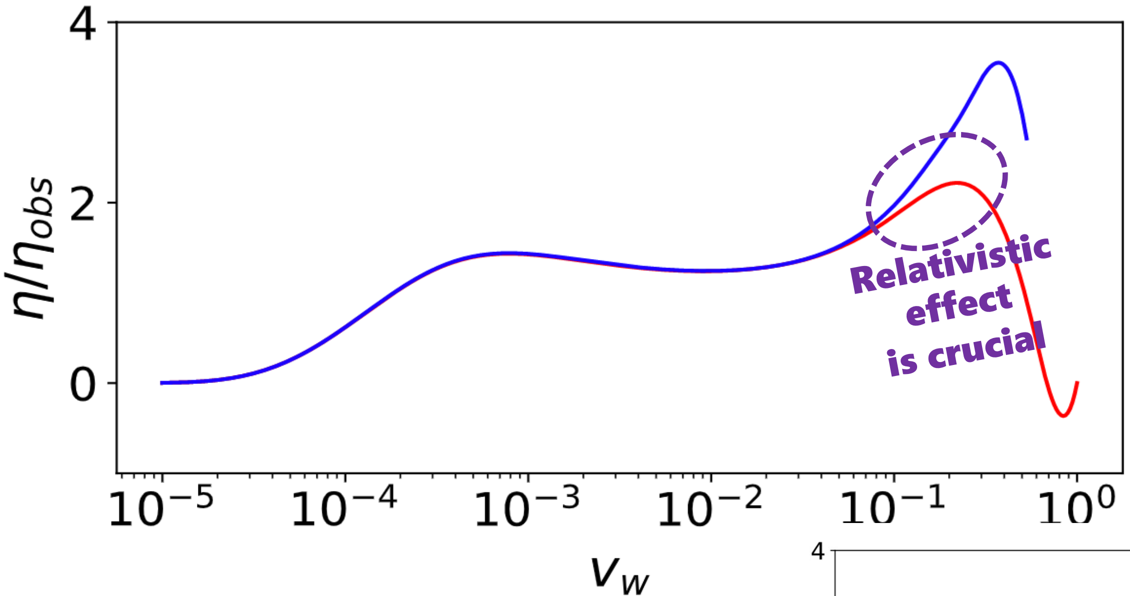

For the predictable GWs,
relativistic effects must be included.

Blue: Fromme and Huber, JHEP 03 (2007)

Red: Cline and Kainulainen, Phys. Rev. D 101 (2020)

Velocity dependences
differ in nucleation temperatures.

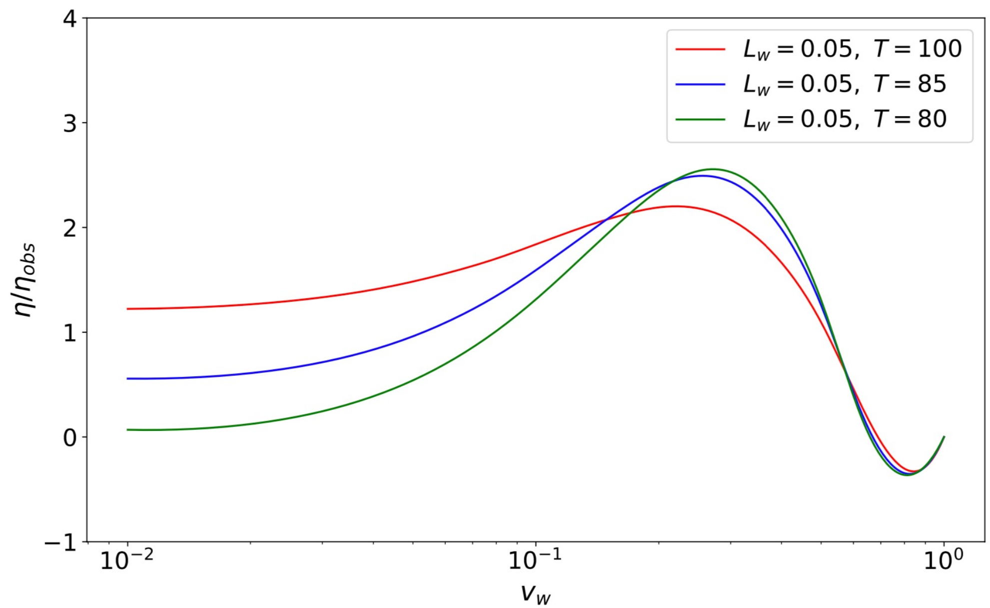

Velocity dep. of efficiency factor

Efficiency $\kappa_v(\alpha, v_w)$ means how much the latent heat is converted to the sound waves.

No hydrodynamical eq. exists when $\alpha \sim 1,\ v_w \lesssim c_s$. Espinosa *et al.* JCAP 06 (2010)

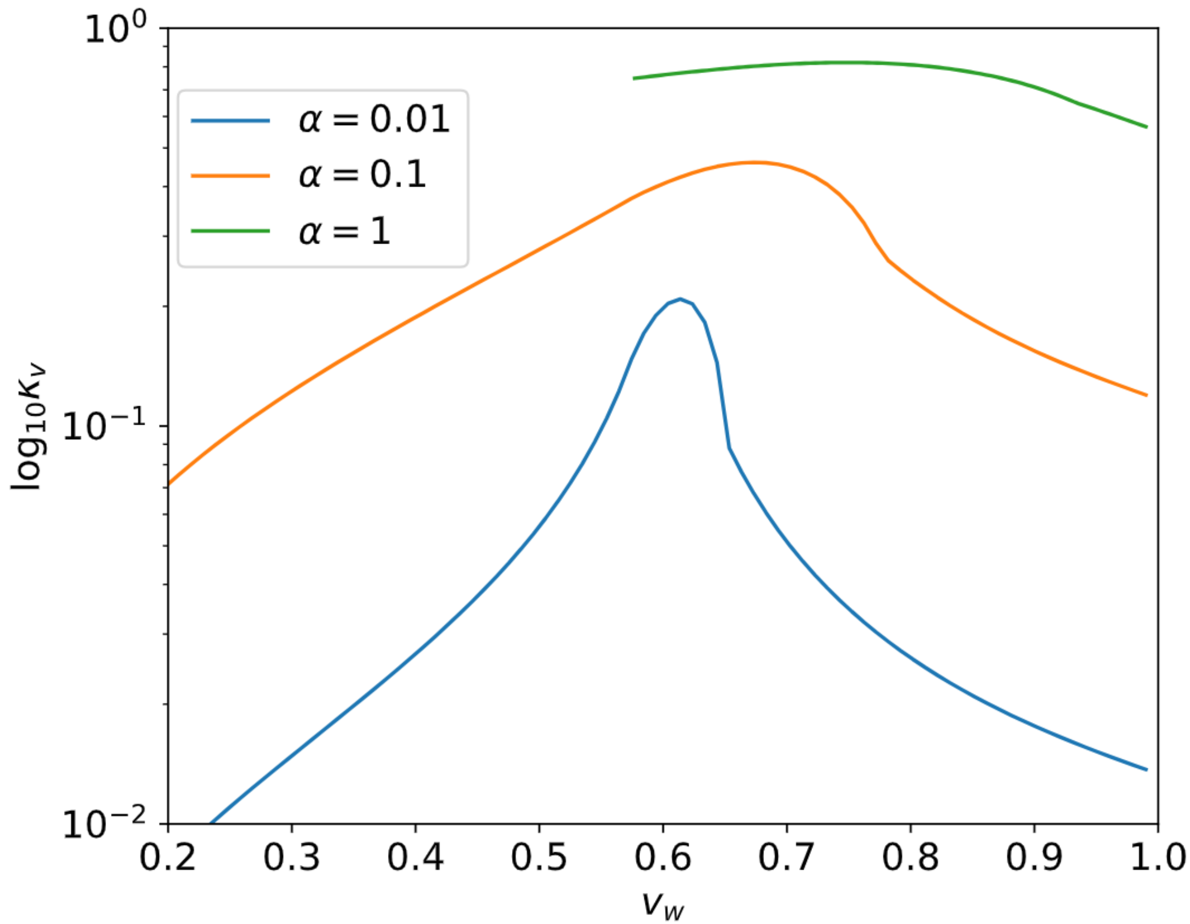

EW Phase transition

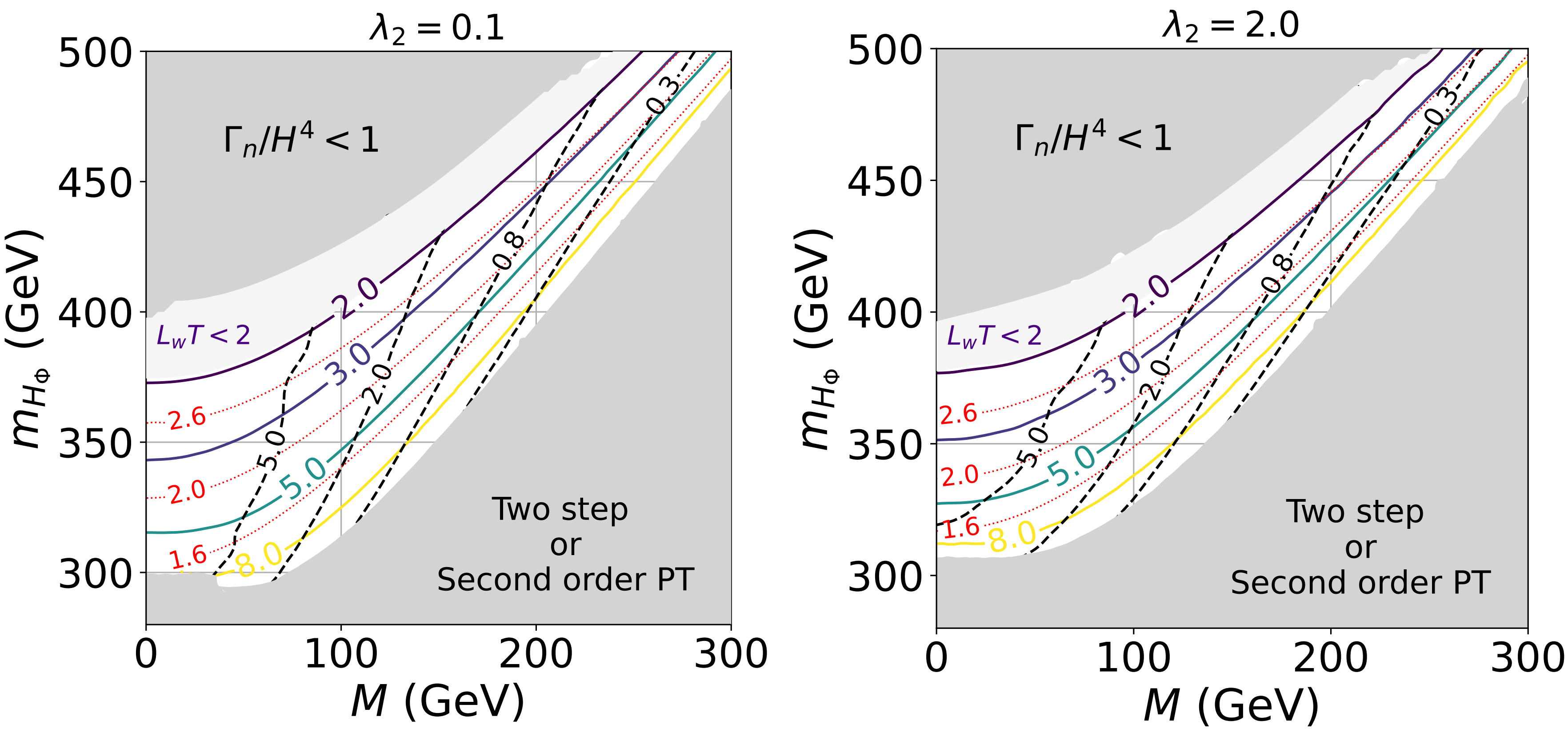

When M and λ_2 are large, $\partial_z\theta|_{max}$ becomes small.

Red dotted : v_n/T_n
Color solid : L_wT
Black dashed : $\partial_z\theta|_{max}$

Source term $\quad S_\theta = -v_w K_8(m^2\theta')' + v_w K_9 \theta' m^2 (m^2)'$

Scatter plot for eEDM and BAU

$$\lambda_2 = 0.1,\ m_\Phi = 350\ \mathrm{GeV},\ M = 30\ \mathrm{GeV},\ v_w = 0.1,$$

$$\theta_u = \theta_d = [0, 2\pi),\ |\zeta_d| = |\zeta_e| = [0, 10],\ |\lambda_7| = [0.5, 1.0],\ \theta_7 = [0, 2\pi).$$

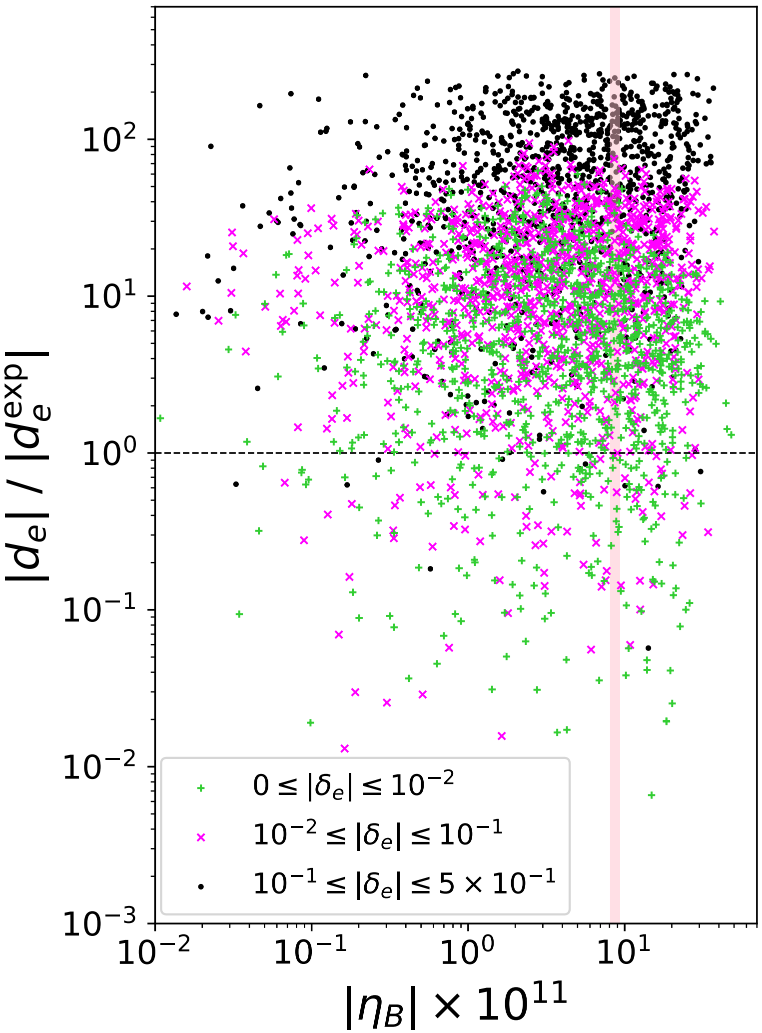

These points are allowed from various constraints.

Fermion loop contributions are proportional to $|\zeta_u||\zeta_e|\sin\delta_e$. $(\delta_e \equiv \theta_u - \theta_e)$

Many points are satisfied from eEDM data and they generate sufficient BAU.

Velocity dependence of BAU

Baryon asymmetry in the relativistic bubble wall velocity Cline and Kainulainen, Phys. Rev. D 101 (2020)

Assuming the velocity as a free parameter

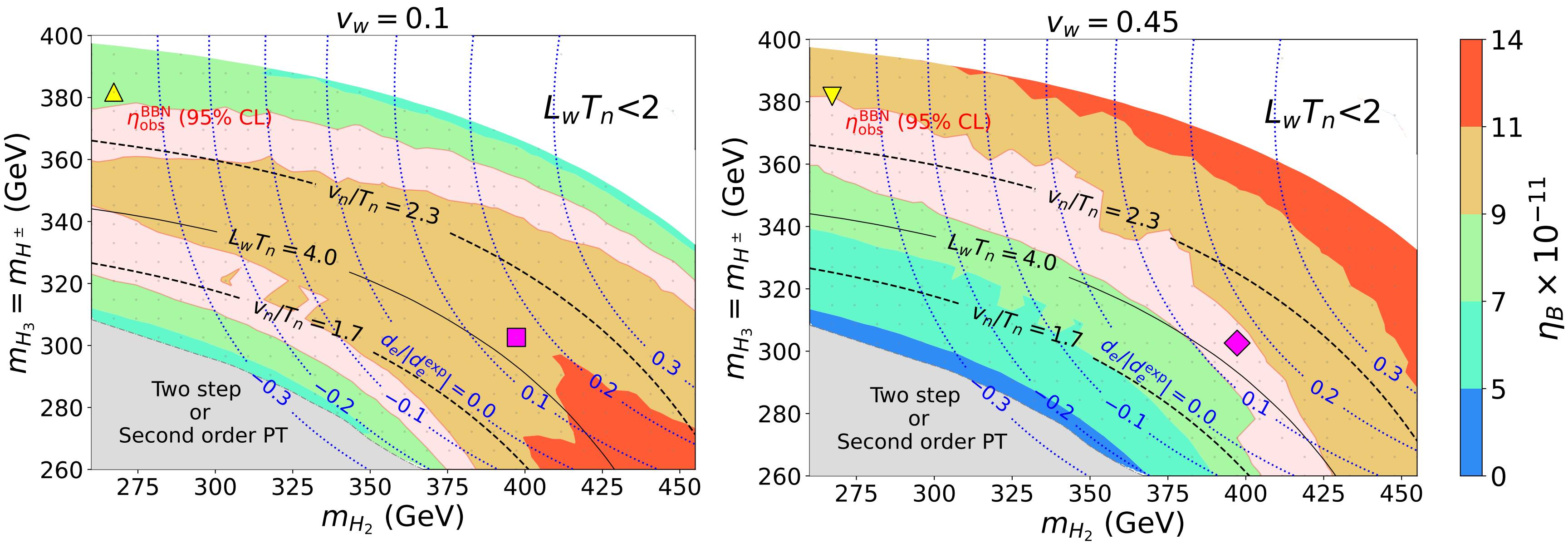

Strongly first order PT (except for gray region)

$M = 30\,\mathrm{GeV},\ \lambda_2 = 0.1,\ |\lambda_7| = 0.8,\ \theta_7 = -0.9,$

$|\zeta_u| = |\zeta_d| = |\zeta_e| = 0.18,\ \theta_u = -2.7,\ \delta_d = 0,\ \delta_e = -0.04.$

The observed BAU (pink) $\eta_{obs}^{\rm BBN} \equiv \dfrac{n_B}{s} = 8.2\text{–}9.2 \times 10^{-11}$

green: relate to the BAU
blue: relate to the eEDM
purple: relate to the both

Electron EDM (blue dotted) $|d_e^{\rm exp}| < 1.1 \times 10^{-29} e$ cm

Andreev *et al.* [ACME] Nature 562 (2018)

We set four benchmarks :

- △ BP1a: small velo. + strongly PT
- ▽ BP1b: large velo. + strongly PT
- □ BP2a: small velo. + weakly PT
- ◇ BP2b: large velo. + weakly PT

Gravitational waves from EWPT

			v_w	m_{H_2}	$m_{H_3,H^\pm}$	M	v_n/T_n	L_wT_n	η_B	ΔR	$\sigma\mathcal{B}(H_1\to\gamma\gamma)$
Strongly PT	small velo. △	BP1a	0.1	267 GeV	381 GeV	30 GeV	2.4	2.6	7.8×10^{-11}	0.61	104 ± 5 fb
	large velo. ▽	BP1b	0.45						9.1×10^{-11}		
Weakly PT	small velo. ◼	BP2a	0.1	397 GeV	302 GeV	30 GeV	2.0	4.1	10.8×10^{-11}	0.44	
	large velo. ◆	BP2b	0.45						9.0×10^{-11}		

Gravitational wave spectra

Grojean and Servant, Phys. Rev. D 75 (2007);
Kakizaki, Kanemura and Matsui, Phys. Rev. D 92 (2015); and more

Sensitivity curves Hashino *et al.* Phys. Rev. D 99 (2019)

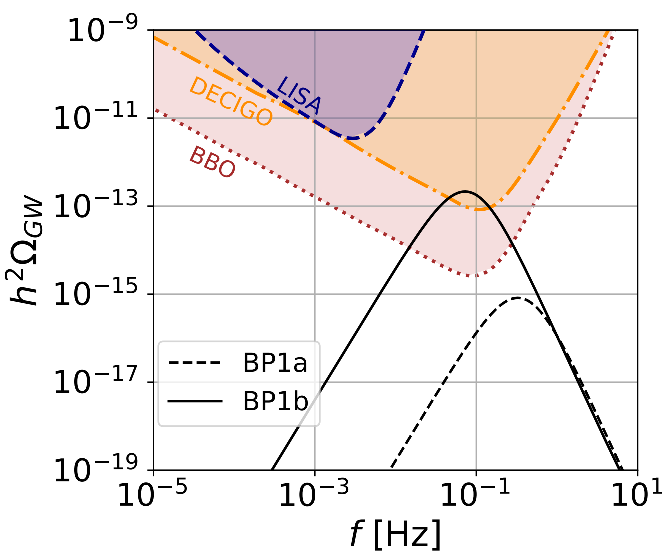

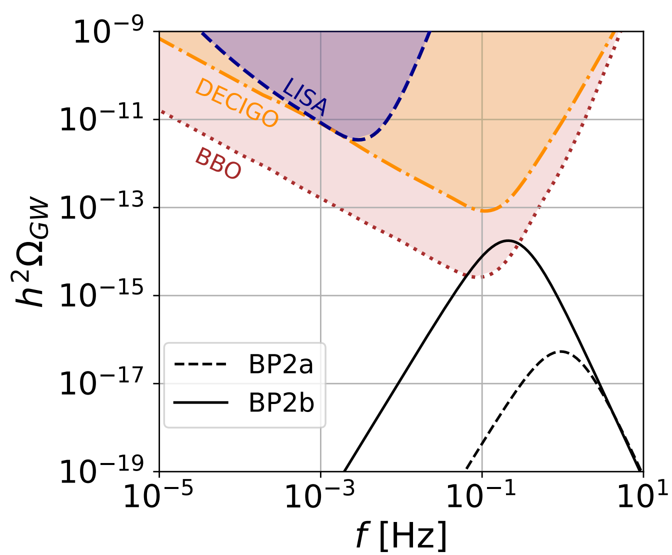

Strong PT and large velocity are needed.

BP1b and BP2b can also be tested by GW observation.

Triple Higgs couplings

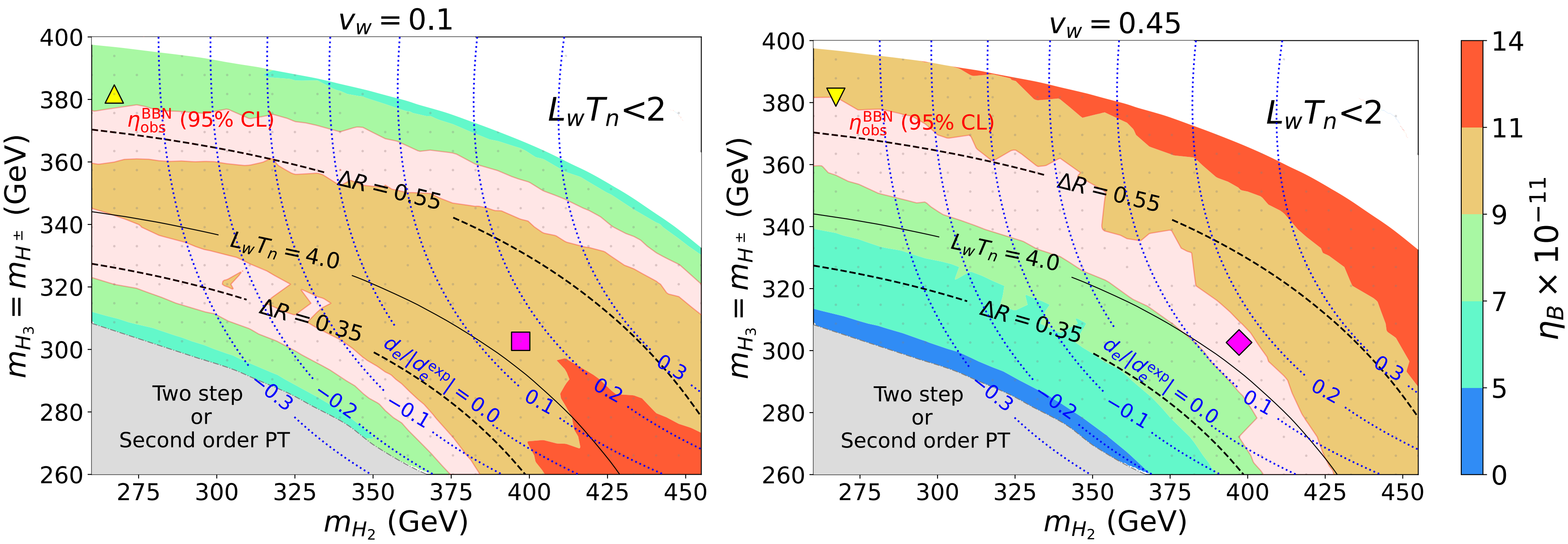

Destructive interference

Dimension 5 effective operator

$$H_{\mathrm{EDM}} = -d_f \frac{\boldsymbol{S}}{|\boldsymbol{S}|} \cdot \boldsymbol{E} \qquad \mathcal{L}_{\mathrm{EDM}} = -\frac{d_f}{2} \overline{f} \sigma^{\mu\nu} (i\gamma_5) f F_{\mu\nu}$$

Time reversal

$$\mathcal{T}(\boldsymbol{E}) = \boldsymbol{E}, \mathcal{T}(\boldsymbol{S}) = -\boldsymbol{S}$$

T violation → From CPT theorem, CP is violated.

Two diagrams contribute to the electron EDM in our model.

Experimental bound $|d_e| < 1.1 \times 10^{-29} e$ cm

Andreev *et al.* [ACME] Nature 562 (2018)

$d_e \simeq$

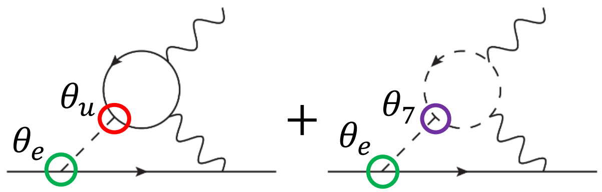

(a) Fermion-loop. (b) Higgs boson-loop.

Destructive interference between two independent CP phase

Kanemura, Kubota and Yagyu, JHEP 08 (2020)

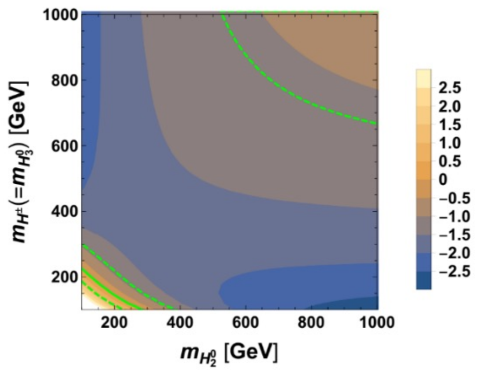

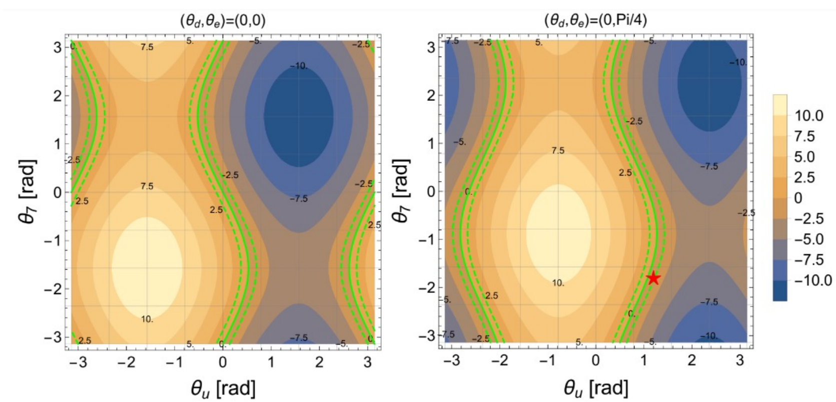

θ_7 and θ_u are important to generate BAU.

Angular distribution

Detection of CP phase θ_e in ILC

Decay process of the heavy neutral scalars $H_{2,3} \to \tau^+\tau^- \to X^+\overline{\nu}X^-\nu$

Kanemura, Kubota and Yagyu, JHEP 04 (2021)

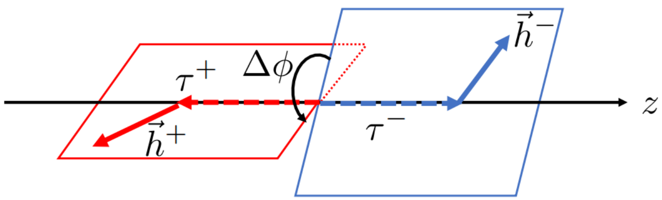

$$\int\int d\cos\theta^- d\cos\theta^+ \overline{|\mathcal{M}(H_2 \to \tau^-\tau^+ \to X^-\nu X^+\overline{\nu})|^2}$$
$$\propto 16 - \pi^2 \cos(2\theta_e - \Delta\phi)$$

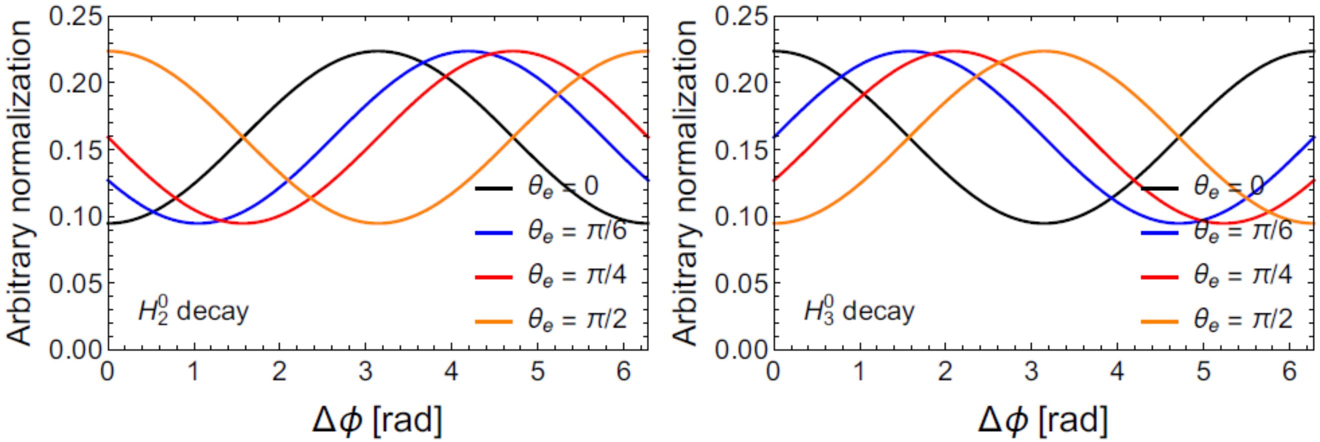

Prospects

More general Yukawa structure

Ex) Down type quark couplings to the heavy scalars

$$y_{d,2} = \zeta_d y_{d,1} \quad \zeta_d \delta_{ij} \to \begin{pmatrix} \zeta_d & & \\ & \zeta_s & \\ & & \zeta_b \end{pmatrix}_{ij}$$

Various possibilities about CPV

- Top
- Top-charm mixing
- Bottom
- Tau
- Tau-mu mixing
- …

Chung (2010)
Chiang *et al.* (2016)
Fuyuto *et al.* (2018)
…

Restrict each scenario

Belle Ⅱ
KOTO
Neutron EDM
Electron EDM
Muon EDM
Tau EDM
…

Ex) Bottom EWBG and B physics   Modak and Senaha, Phys. Rev. D 99 (2019)

Blue: $\eta_B / \eta_B^{obs} = 1$

Red: ΔA_{CP} (Belle Ⅱ)

Green: $B \to s\gamma$ (Belle Ⅱ)

Left (Right): Central value is the SM (Current) one

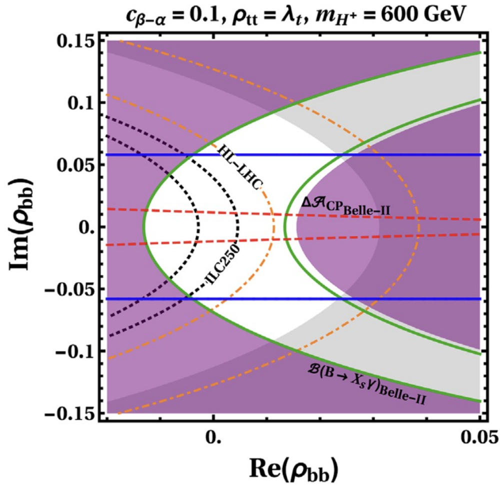

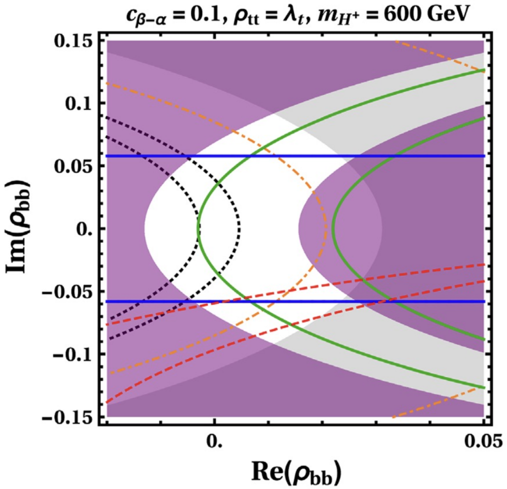

Effective potential

Thermal resummation → Parwani scheme
1 loop potential → Landau gauge ($\xi = 0$)

Renormalization condition
→ MS-bar scheme ($\lambda_{2,7}, M$) + On-shell scheme (other parameters)

$$\left.\frac{\partial V}{\partial h_i}\right|_{\substack{h_1=v\\ h_2=h_3=0}} = 0$$

$$\left.\frac{\partial^2 V}{\partial h_i \partial h_j}\right|_{\substack{h_1=v\\ h_2=h_3=0}} = \mathcal{M}_{ij}^2$$

We used cutoff $m_{NG} = m_{IR} \sim 1$ GeV to avoid IR divergence.

Higgs triple coupling at 1 loop level

$$\Delta R \equiv \frac{\lambda_{hhh} - \lambda_{hhh}^{\rm SM}}{\lambda_{hhh}^{\rm SM}}$$
$$\simeq \frac{1}{12\pi^2 v^2 m_{H_1}^2}\left\{2\frac{(m_\pm^2 - M^2)^3}{m_\pm^2} + \frac{(m_{H_2}^2 - M^2)^3}{m_{H_2}^2} + \frac{(m_{H_3}^2 - M^2)^3}{m_{H_3}^2}\right\}$$

Relation between ϕ/T and ΔR (right figure)

K. Enomoto, S. Kanemura, and Y.M, JHEP 01 (2022) 104

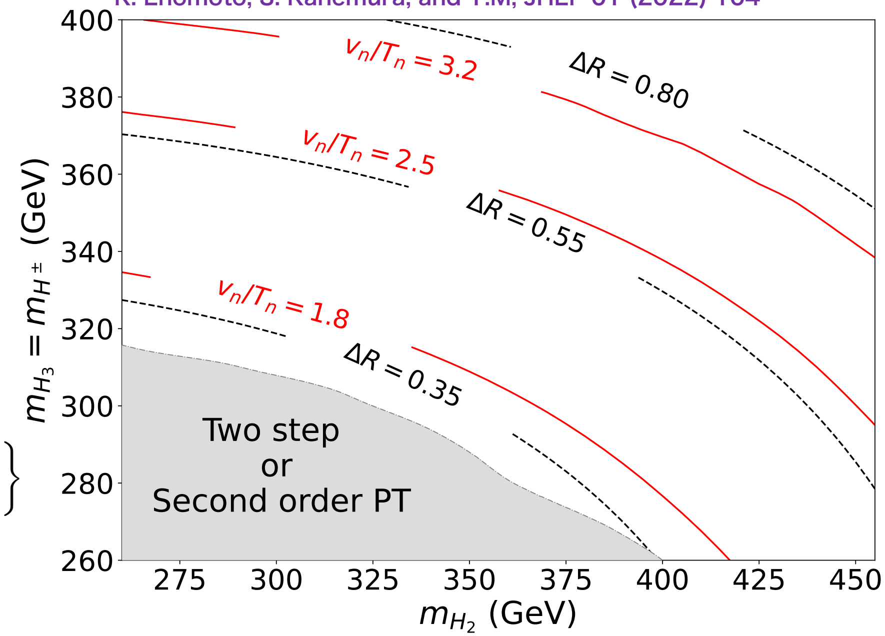

CP violating bubble

Order parameter $h_1 = h, h_2 = H\cos\varphi_H, h_3 = H\sin\varphi_H$

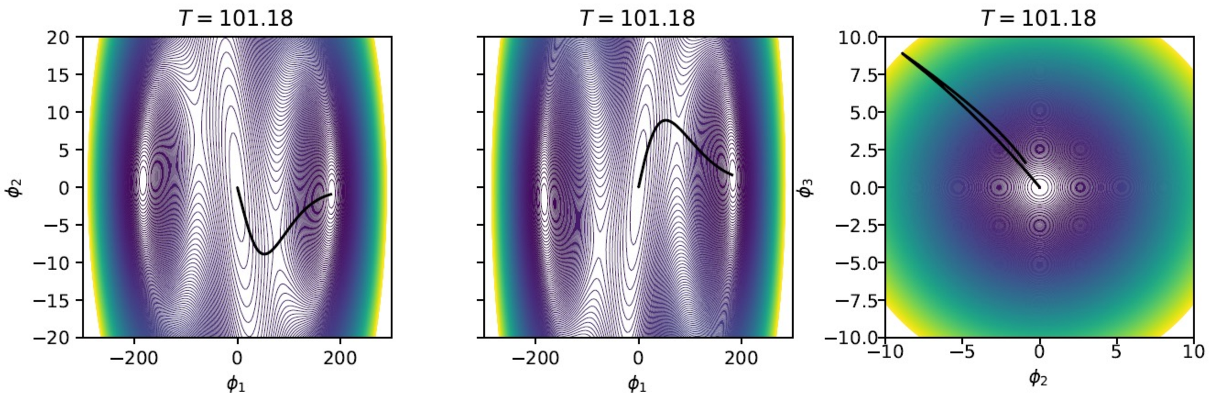

Black line is the path of PT.

Vertical: Heavy scalar mode
Horizontal: Light scalar mode

Large VEVs $\phi_{2,3}$ during PT are needed for BAU.

Localized top phase

$$\partial_z\theta(z) = -\frac{\varphi_H^2}{\varphi_{H_1}^2 + \varphi_H^2}\partial_z\theta_H - \partial_z \arctan\left(\frac{|\zeta_u|\varphi_H \sin(\theta_H + \theta_u)}{\varphi_{H_1} + |\zeta_u|\varphi_H \cos(\theta_H + \theta_u)}\right),$$

$$\varphi_H \equiv \sqrt{\varphi_{H_2}^2 + \varphi_{H_3}^2}, \quad \theta_H = \arctan(\varphi_{H_2}/\varphi_{H_3}),$$

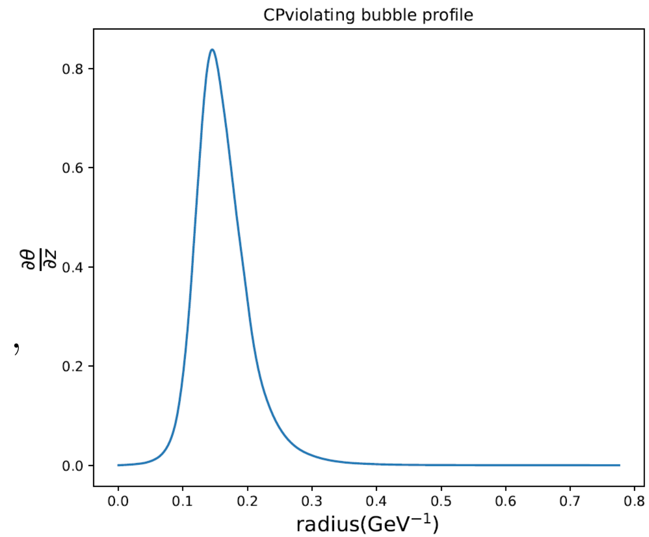

We used `CosmoTransitions` to calculate the bubble wall profile.

Wainwright, Comput. Phys. Commun. 183 (2011)

Estimation of baryon density

<u>Top transport scenario</u> Fromme and Huber, JHEP 03 (2007)

CP violating source is the top quark which has large yukawa coupling.

Localized top quark mass $$m_t(z) = \frac{y_t}{\sqrt{2}} v(z) e^{i\theta(z)}$$

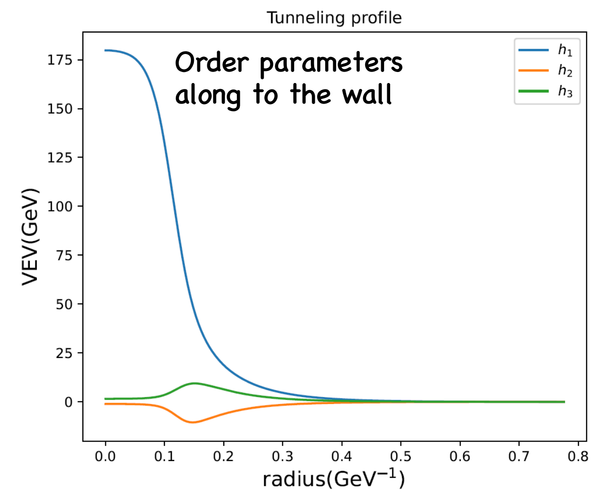

Higgs potential at finite temperature determines the bubble profile.

$v(z), \theta(z), T_n, L_w, \ldots$

"Semi classical force mechanism" (WKB method) Cline, Joyce and Kainulainen, JHEP 07 (2000); Cline and Kainulainen Phys. Rev. D 101 (2020)

Boltzmann equation $$(\partial_t + \boldsymbol{v}_g \cdot \partial_{\boldsymbol{x}} + \boldsymbol{F} \cdot \partial_{\boldsymbol{p}}) f_i = C[f_i, f_j, \ldots]$$

Overall signs are flipped between particles and anti-particles.

$$v_g = \frac{p_z}{E_0}\left(1 \pm s\frac{\theta'}{2}\frac{m^2}{E_0^2 E_{0z}}\right)$$

$$F_z = -\frac{(m^2)'}{2E_0} \pm s\frac{(m^2\theta')'}{2E_0 E_{0z}} \mp s\frac{\theta' m^2 (m^2)'}{4E_0^3 E_{0z}}$$

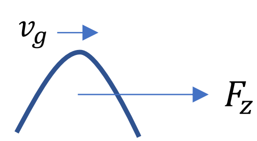

WKB wave packet

Particle distributions are small away from its equilibrium form

$$f_i = \frac{1}{e^{\beta[\gamma_w(E_i + v_w p_z) - \mu_i]} \pm 1} + \delta f_i$$

Transport equations

Boltzmann equation $(\partial_t + \boldsymbol{v}_g \cdot \partial_{\boldsymbol{x}} + \boldsymbol{F} \cdot \partial_{\boldsymbol{p}}) f_i = C[f_i, f_j, \ldots]$

$$v_g = \frac{p_z}{E_0}\left(1 \pm s\frac{\theta'}{2}\frac{m^2}{E_0^2 E_{0z}}\right)$$

$$F_z = -\frac{(m^2)'}{2E_0} \pm s\frac{(m^2\theta')'}{2E_0 E_{0z}} \mp s\frac{\theta' m^2 (m^2)'}{4E_0^3 E_{0z}}$$

Overall signs are flipped between particle and anti-particle.

Particle distributions are small away from its equilibrium form $f_i = \frac{1}{e^{\beta[\gamma_w(E_i + v_w p_z) - \mu_i]} \pm 1} + \delta f_i$

Boltzmann equation can be expanded by small wall velocity, and after integrated in momentum,

$$v_w K_1 \mu' + v_w K_2 (m^2)' \mu + u' - \langle \boldsymbol{C}[f] \rangle = 0$$

(K series are z-dependent functions)

$$-K_4 \mu' + v_w \tilde{K}_5 u' + v_w \tilde{K}_6 (m^2)' u - \left\langle \frac{p_z}{E_0} \boldsymbol{C}[f] \right\rangle = S_\theta$$

$$S_\theta = -v_w K_8 (m^2 \theta')' + v_w K_9 \theta' m^2 (m^2)'$$

Plasma flame

$$\frac{\partial n_B}{\partial t} = \frac{3}{2}\Gamma_{\mathrm{sph}}\left(3\mu_{B_L} - \frac{A}{T^3} n_B\right)$$

Integrated in wall flame

$$\eta_B = \frac{405\Gamma_{\mathrm{sph}}}{4\pi^2 v_w g_* T}\int_0^\infty dz\ \mu_{B_L} f_{\mathrm{sph}} e^{-45\Gamma_{\mathrm{sph}} z/(4v_w)}$$

$$f_{\mathrm{sph}}(z) = \min\left(1, \frac{2.4T}{\Gamma_{\mathrm{sph}}} e^{-40v(z)/T}\right)$$

Higgs triple coupling

de Blas *et al.* JHEP 01(2020)

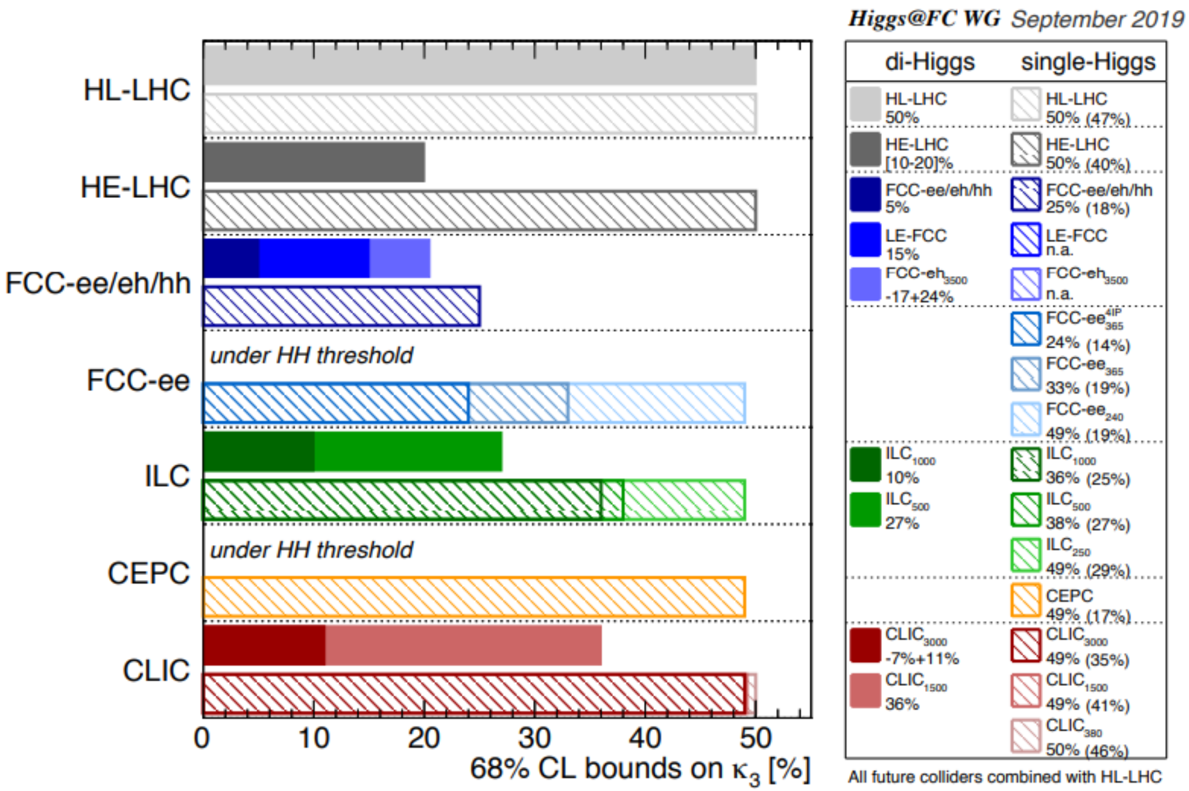

Hadron collider

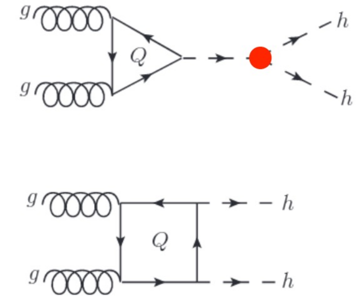

Lepton collider

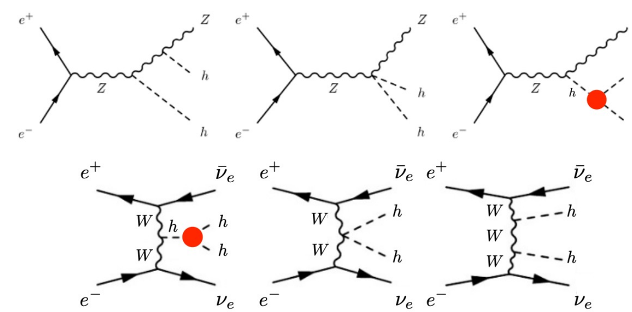

Higgs to di-photon decay

Non decoupling effect in $H_1 \to \gamma\gamma$

The constraints on the coupling $H_1 H^{\pm} H^{\pm}$

$$m_{H^{\pm}}^2 = M^2 + \frac{1}{2}\lambda_3 v^2$$

Red line is prediction in the case of $M = 30$ GeV.

SM expected (blue): $\sigma Br(H_1 \to \gamma\gamma) = 116 \pm 5$ fb

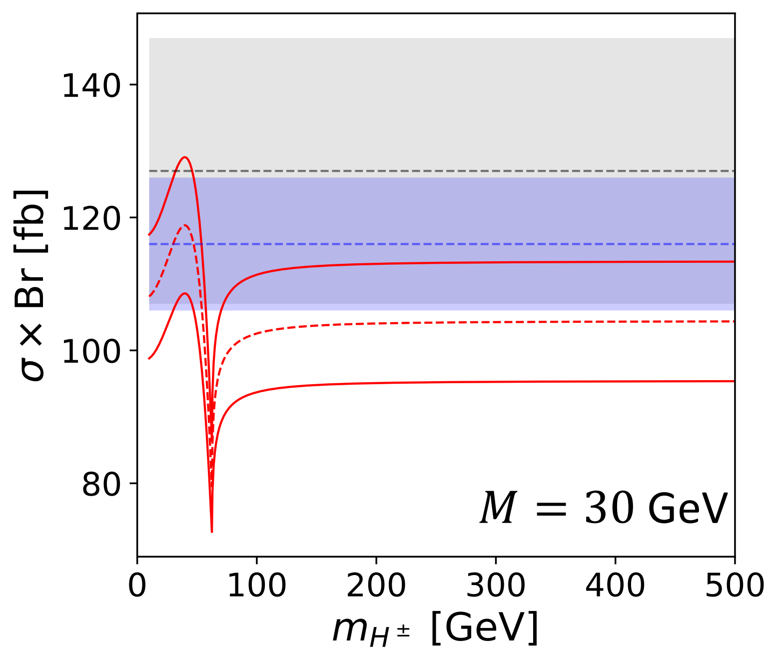

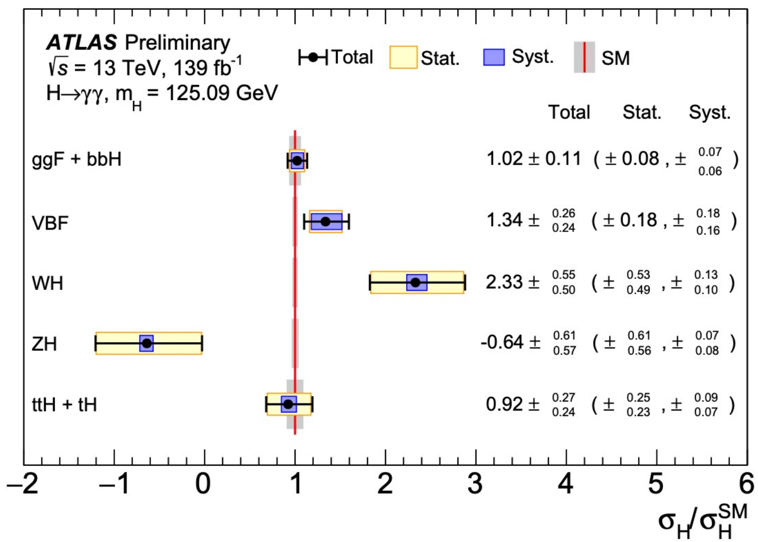

Observed (gray): $\sigma Br(H_1 \to \gamma\gamma) = 127 \pm 10$ fb

σ is inclusive production cross section of H_1.

ATLAS-CONF-2020-026

Other constraints

STU parameter

Considering Higgs alignment and $m_{H_3} = m_{H^\pm}$, our potential has custordial symmetry at 1 loop level.

$$
\begin{aligned}
V =& -\frac{1}{2}\mu_1^2 \mathrm{Tr}(M_1^\dagger M_1) - \frac{1}{2}\mu_2^2 \mathrm{Tr}(M_2^\dagger M_2) - \mu_{3R}^2 \mathrm{Tr}(M_1^\dagger M_2) + \mu_{3I}^2 \mathrm{Tr}(M_1^\dagger M_2 \tau_3) \\
&+ \frac{1}{8}\lambda_1 \mathrm{Tr}^2(M_1^\dagger M_1) + \frac{1}{8}\lambda_2 \mathrm{Tr}^2(M_2^\dagger M_2) + \frac{1}{4}\lambda_3 \mathrm{Tr}(M_1^\dagger M_1)\mathrm{Tr}(M_2^\dagger M_2) \\
&+ \frac{1}{2}\lambda_{5R} \mathrm{Tr}^2(M_1^\dagger M_2) + \frac{1}{4}(\lambda_4 - \lambda_{5R})\left(\mathrm{Tr}^2(M_1^\dagger M_2) - \mathrm{Tr}^2(M_1^\dagger M_2\tau_3)\right) + \frac{1}{2}\lambda_{5I} \mathrm{Tr}(M_1^\dagger M_2)\mathrm{Tr}(M_1^\dagger M_2 \tau_3) \\
&+ \lambda_{6R} \mathrm{Tr}(M_1^\dagger M_1)\mathrm{Tr}(M_1^\dagger M_2) + \lambda_{6I} \mathrm{Tr}(M_1^\dagger M_1)\mathrm{Tr}(M_1^\dagger M_2 \tau_3) \\
&+ \lambda_{7R} \mathrm{Tr}(M_2^\dagger M_2)\mathrm{Tr}(M_1^\dagger M_2) + \lambda_{7I} \mathrm{Tr}(M_2^\dagger M_2)\mathrm{Tr}(M_1^\dagger M_2 \tau_3)
\end{aligned}
$$

Pomarol and Vega, Nucl. Phys. B 413 (1994)

→ T = 0

S and U parameter in general CPV 2HDM Haber and Neil, Phys. Rev. D 83 (2011)

→ S and U are very small in our benchmark scenario.

Bounded from below

Ferreira, Santos and Barroso, Phys. Lett. B 603 (2004)

$$
\lambda_1 \geq 0, \quad \lambda_2 \geq 0
$$

$$
\lambda_3 \geq -\sqrt{\lambda_1\lambda_2}, \quad \lambda_3 + \lambda_4 \mp \lambda_{5R} \geq -\sqrt{\lambda_1\lambda_2}
$$

$$
|\lambda_{7R}| \leq \frac{1}{4}(\lambda_1 + \lambda_2) + \frac{1}{2}(\lambda_3 + \lambda_4 + \lambda_{5R})
$$

$$
|\lambda_{7I}| \leq \frac{1}{4}(\lambda_1 + \lambda_2) + \frac{1}{2}(\lambda_3 + \lambda_4 - \lambda_{5R})
$$

Unitarity bound (M = 30 GeV)

Kanemura and Yagyu, Phys. Lett. B 751 (2015)

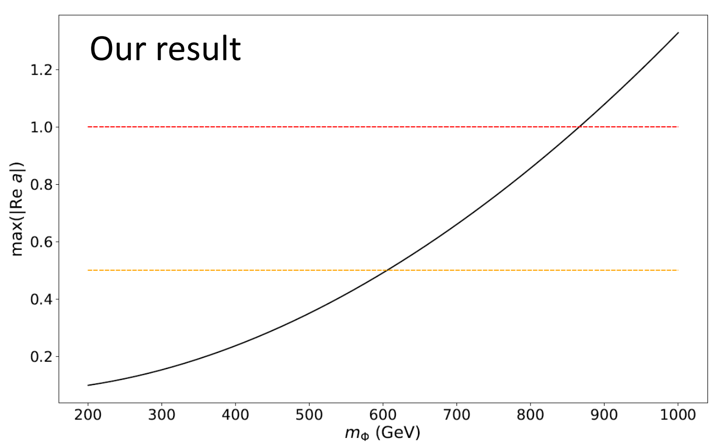

Shape of the chemical potential

When the top transport scenario, θ_7 and θ_u are important for the BAU.

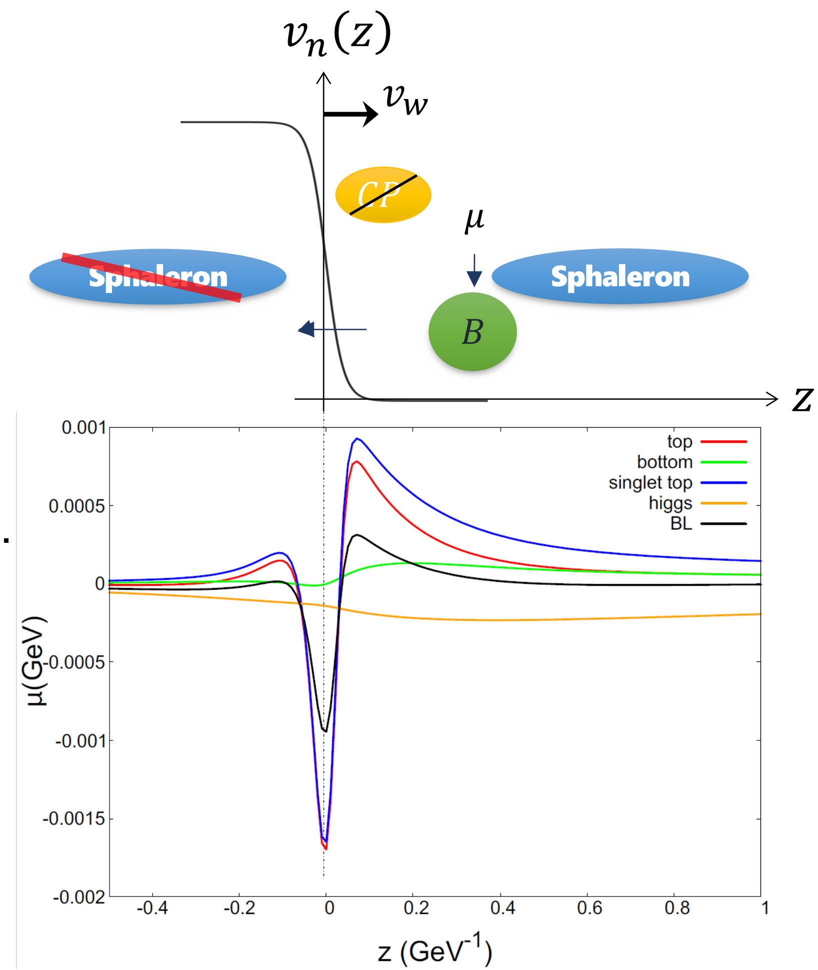

Localized mass around the wall

$$m_t(z) = \frac{y_t}{\sqrt{2}} v(z) e^{i\theta(z)}$$

makes chemical potential.

$v(z), \theta(z), T_n$, etc.
depend on models and dynamics of PT.

Wall width dependence of BAU

Cline and Laurent, Phys. Rev. D 104 (2021)

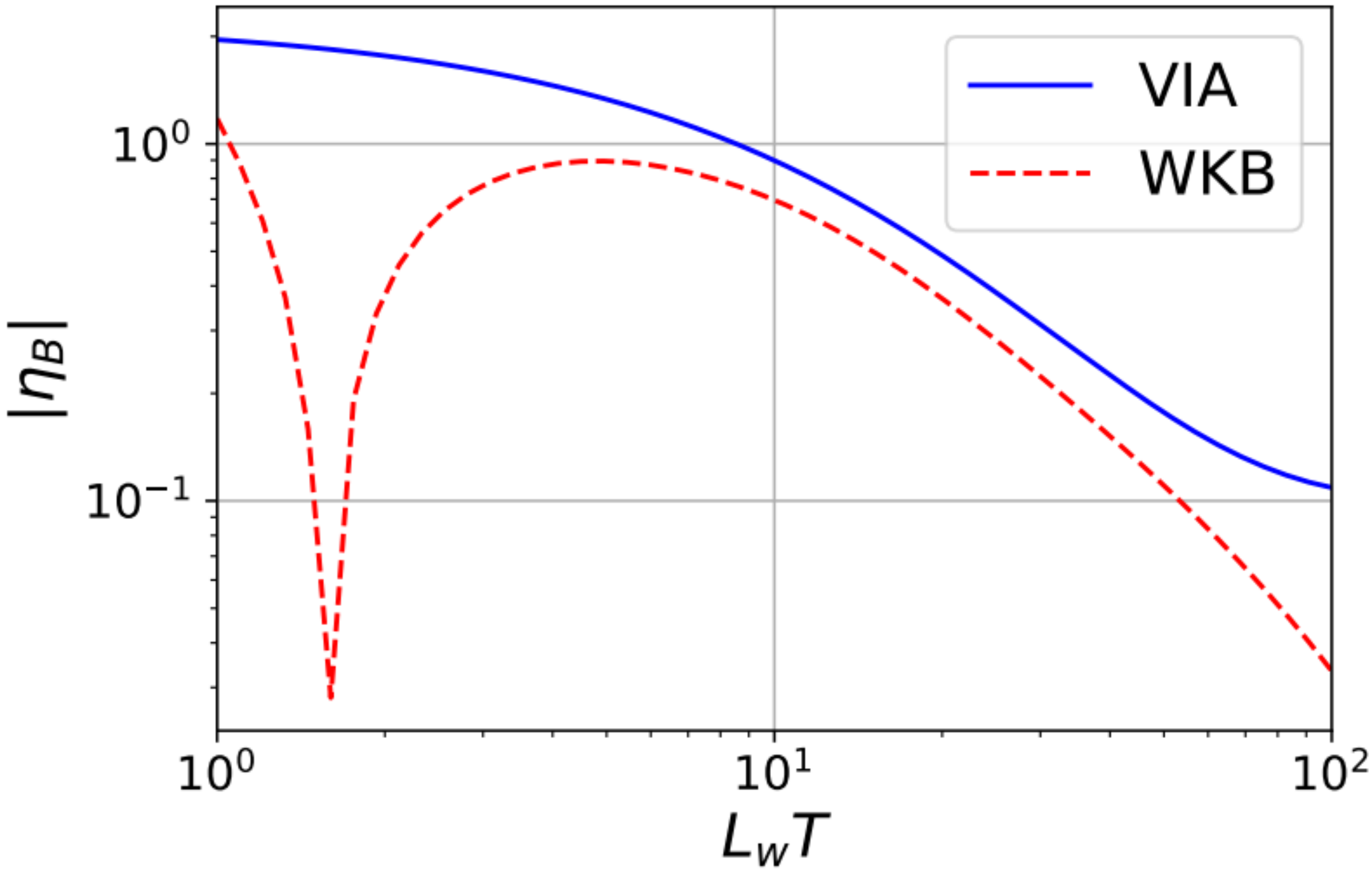

WKB formalism has accidental zero-crossing behavior.

Triviality bound 1

Scalar coupling often diverge by non-decoupling effect. $m_H \simeq \lambda v^2 + M^2 \gg M^2$

In BP, the largest coupling $\lambda \sim 3$,
Landau pole appears around 1-3 TeV when couplings are run from Z boson scale.

Cline, Kainulainen and Trott, JHEP 11 (2011)

However, the scale of Landau pole depends on whether threshold effects are considered.

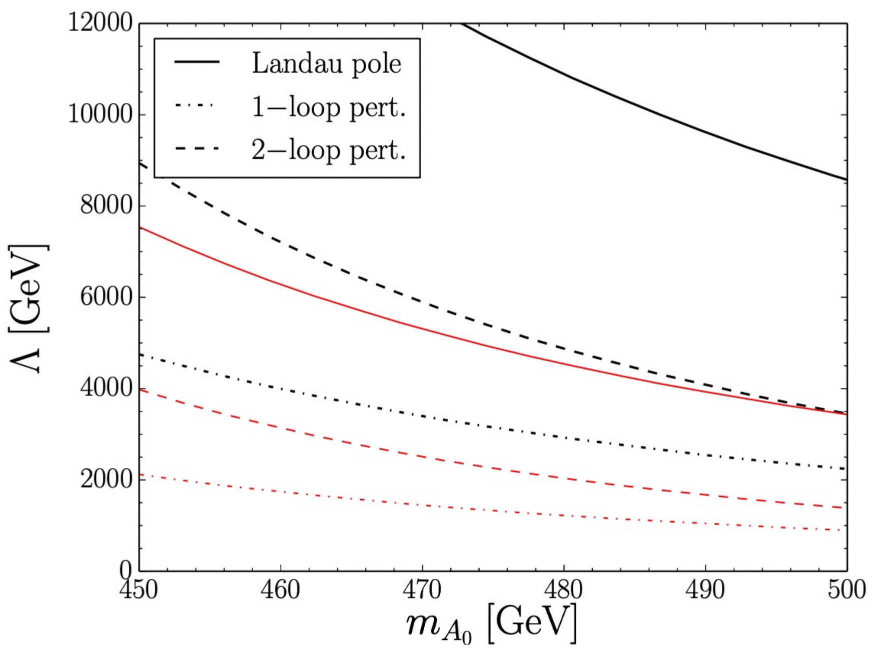

The largest coupling $\lambda \sim 7$

Effects of heavy particles are included at

μ ~200 GeV (black)
μ ~500 GeV (red)

Dorsch, Huber, Konstandin and No, JCAP 05 (2017)

Triviality bound 2

Our result (preliminary)

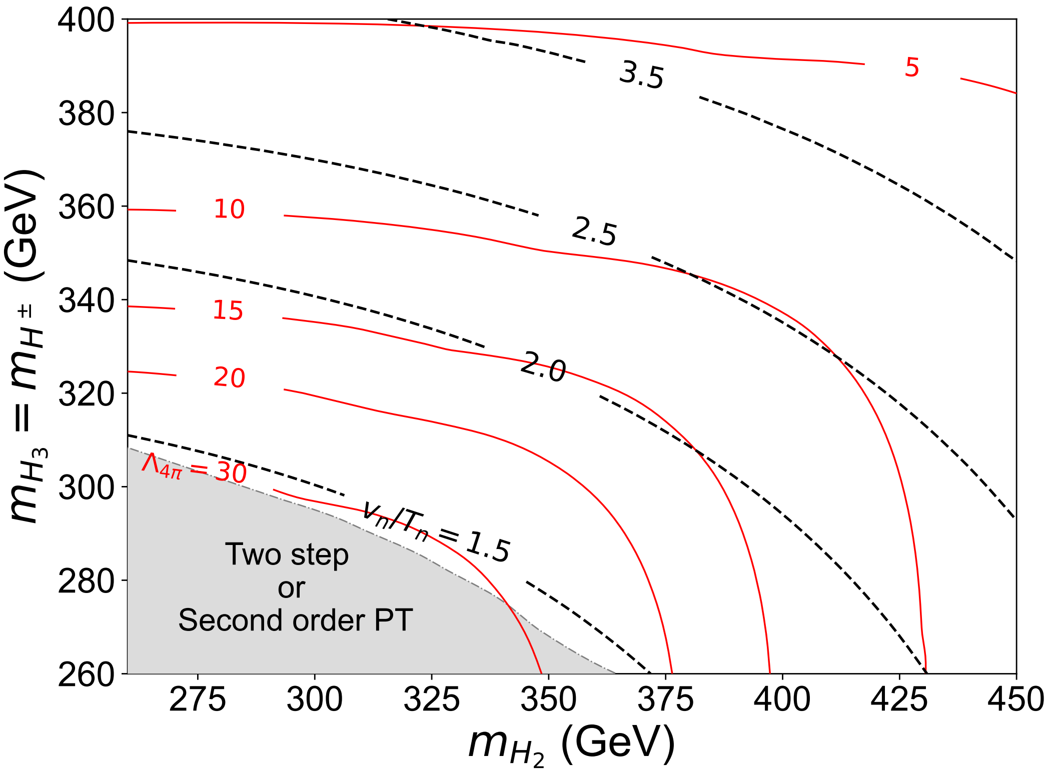

Couplings at BP1

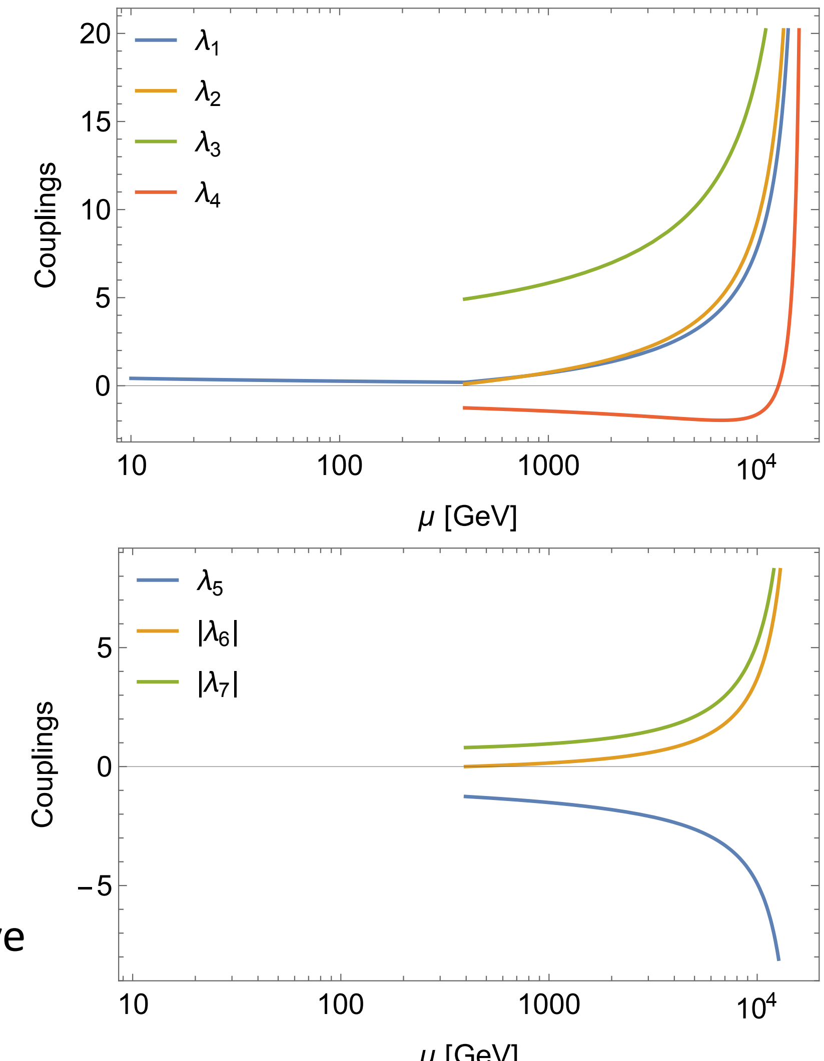

We consider threshold effect at $\mu = \max\{m_{H_2}, m_{H^\pm}\}$.

$\Lambda_{4\pi}$ (TeV) : Where couplings become non-perturbative

Λ_∞ (TeV) : Landau pole

Triviality bound 3

Our result (preliminary)

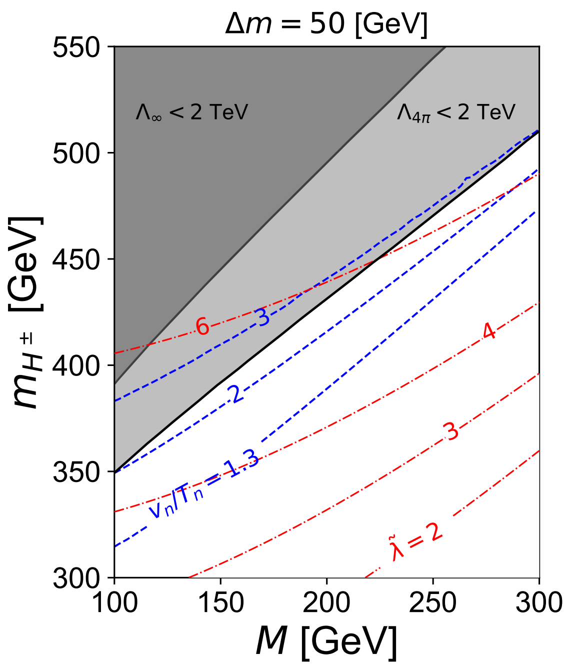

$$\Delta m \equiv m_{H_2} - m_{H^\pm}$$

$$\tilde{\lambda} \equiv \lambda_3 + \lambda_4$$

We set matching scale $\mu = M$.

Below 2 TeV, couplings…

become non-perturbatively (gray)

has Landau pole (dark gray)

Upper bound

$m_{H^\pm} \lesssim 400$ GeV

To obtain sufficient BAU, small M is needed !

(see the slide “CP-violating bubble”)

$v_w = 0.1$

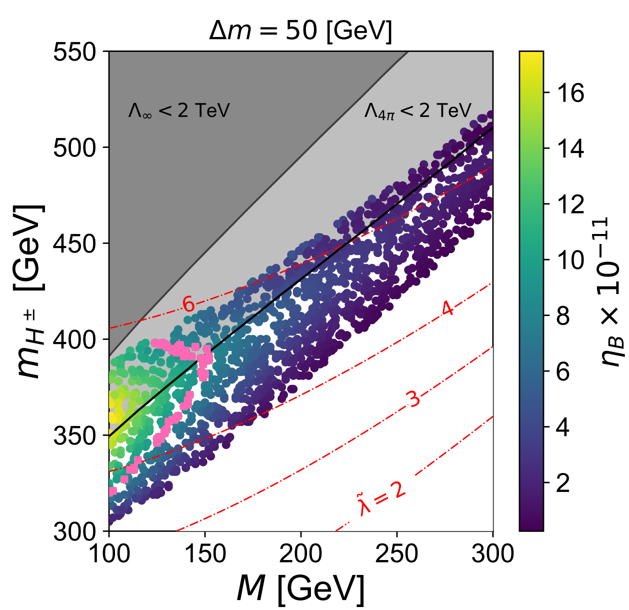

$v_w = 0.4$

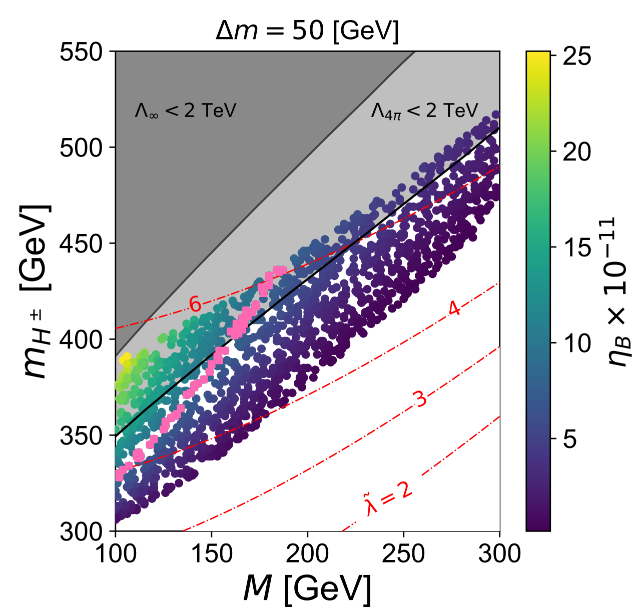

Inputs : same as BP1 and BP2 except for $|\zeta_u| = 0.5, |\lambda_7| = 1.2$

Mass dep. beta function

Consider Gell-Man-Low renormalization group equation.

Ex.) $\lambda\phi^4$ theory

Renormalization conditions

$$\Gamma^{(2)}(p^2 = m^2, m^2, \lambda; Q^2) = 0,$$

⇨ Parameter m become physical mass

$$\frac{\partial}{\partial p^2}\Gamma^{(2)}(p^2, m^2, \lambda; Q^2)_{p^2=-Q^2} = 1,$$

$$\Gamma^{(4)}(p_i, m^2, \lambda; Q^2)_{p_i\cdot p_j = -Q^2\delta_{ij}+\frac{1}{3}Q^2(1-\delta_{ij})} = -\lambda.$$

⇨ Momentum subtraction scheme

Mass dependent beta function

$$\beta(\lambda, m/Q) = \frac{3\lambda^2}{16\pi^2}\cdot \underbrace{\frac{4}{3}\frac{Q^2}{m^2}\int_0^1 dx\, \frac{x(1-x)}{1+\frac{4}{3}\frac{Q^2}{m^2}x(1-x)}}_{\equiv f(Q/m)},$$

$\equiv f(Q/m)$ (right figure)

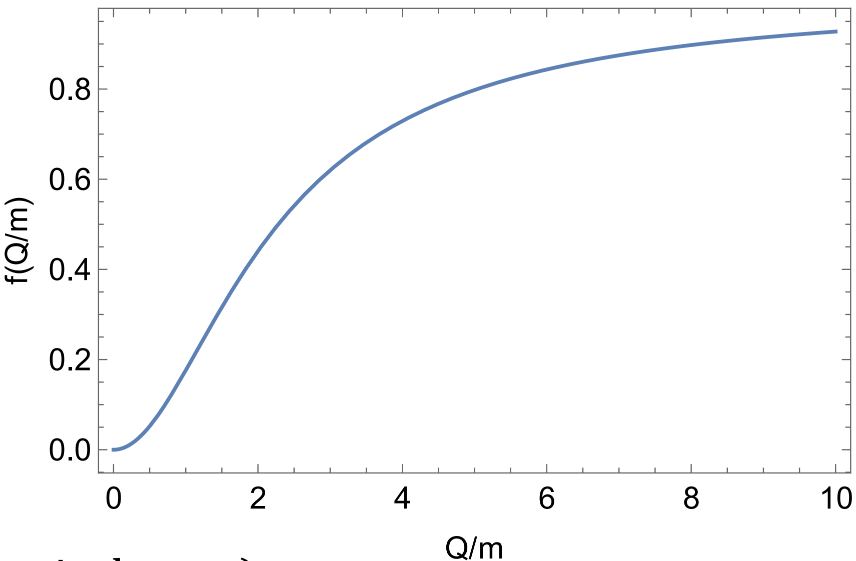

Threshold effects should be included at $\mu \sim (2 \times \text{physical mass})$

RGE analysis in previous work

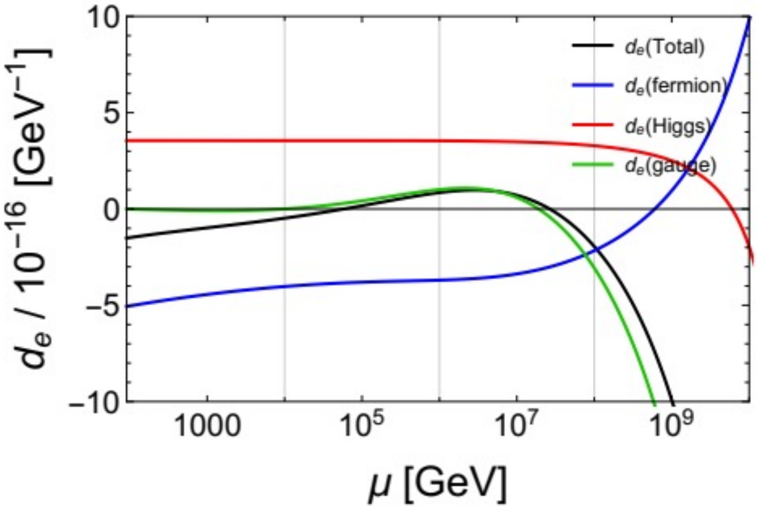

$M = 240,$	$m_{H_2^0} = 280,$	$m_{H_3^0} = 230,$	$m_{H^\pm} = 230$	(in GeV).
$\lvert\zeta_u\rvert = 0.01,$	$\lvert\zeta_d\rvert = 0.1,$	$\lvert\zeta_e\rvert = 0.5,$	$\lvert\lambda_7\rvert = 0.3,$	$\lambda_2 = 0.5.$
$\theta_u = 1.2,$	$\theta_d = 0,$	$\theta_e = \pi/4,$	$\theta_7 = -1.8$	(in rad).

Kanemura, Kubota and Yagyu, JHEP 08 (2020)

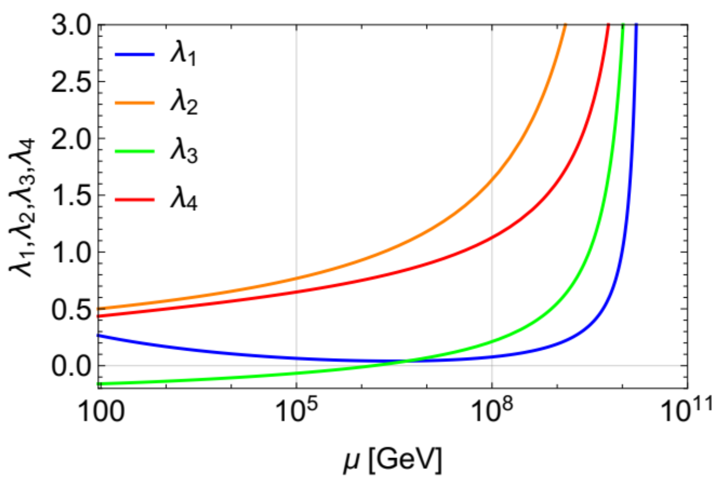

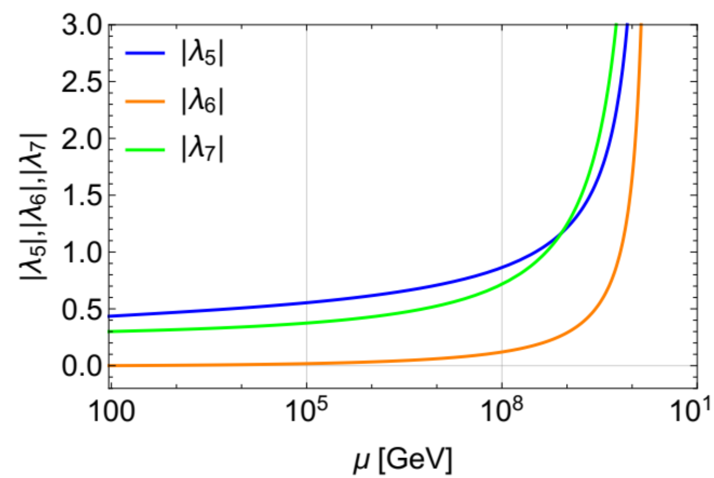

Direct detections

Kanemura, Takeuchi and Yagyu, Phys. Rev. D 105 (2022)

$\zeta_u = 0.1$ case

Orange: $B \to X_s + \gamma$
Magenta: $B_s \to \mu\mu$
Cyan: leptonic tau decay
Black shaded: $H \to \tau\tau$
Black curves: multi lepton search

330 GeV

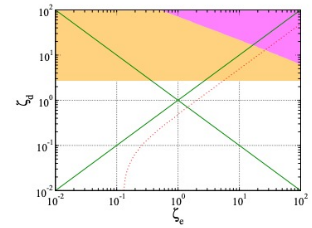

280 GeV

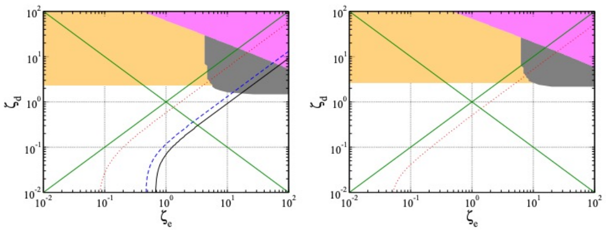

230 GeV

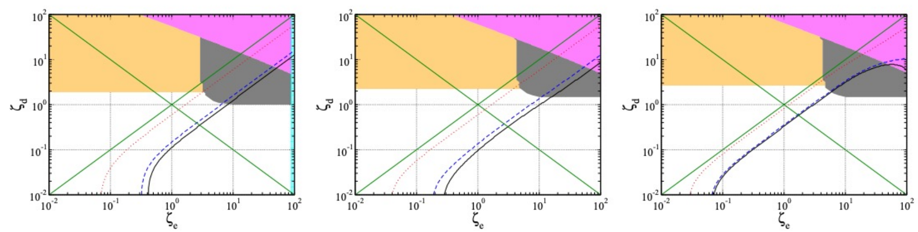

$m_{H_2} = 180$ GeV

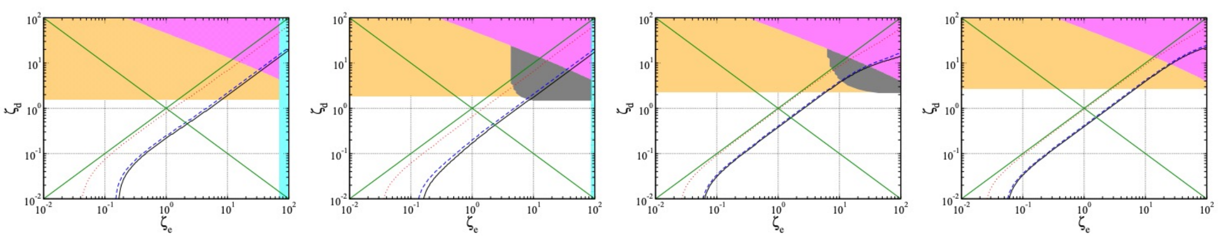

$m_{H_3} = m_{H^\pm} = 180$ GeV | 230 GeV | 280 GeV | 330 GeV

eEDM and BAU in L7 plane

K. Enomoto, S. Kanemura, and Y.M, JHEP 01 (2022) 104

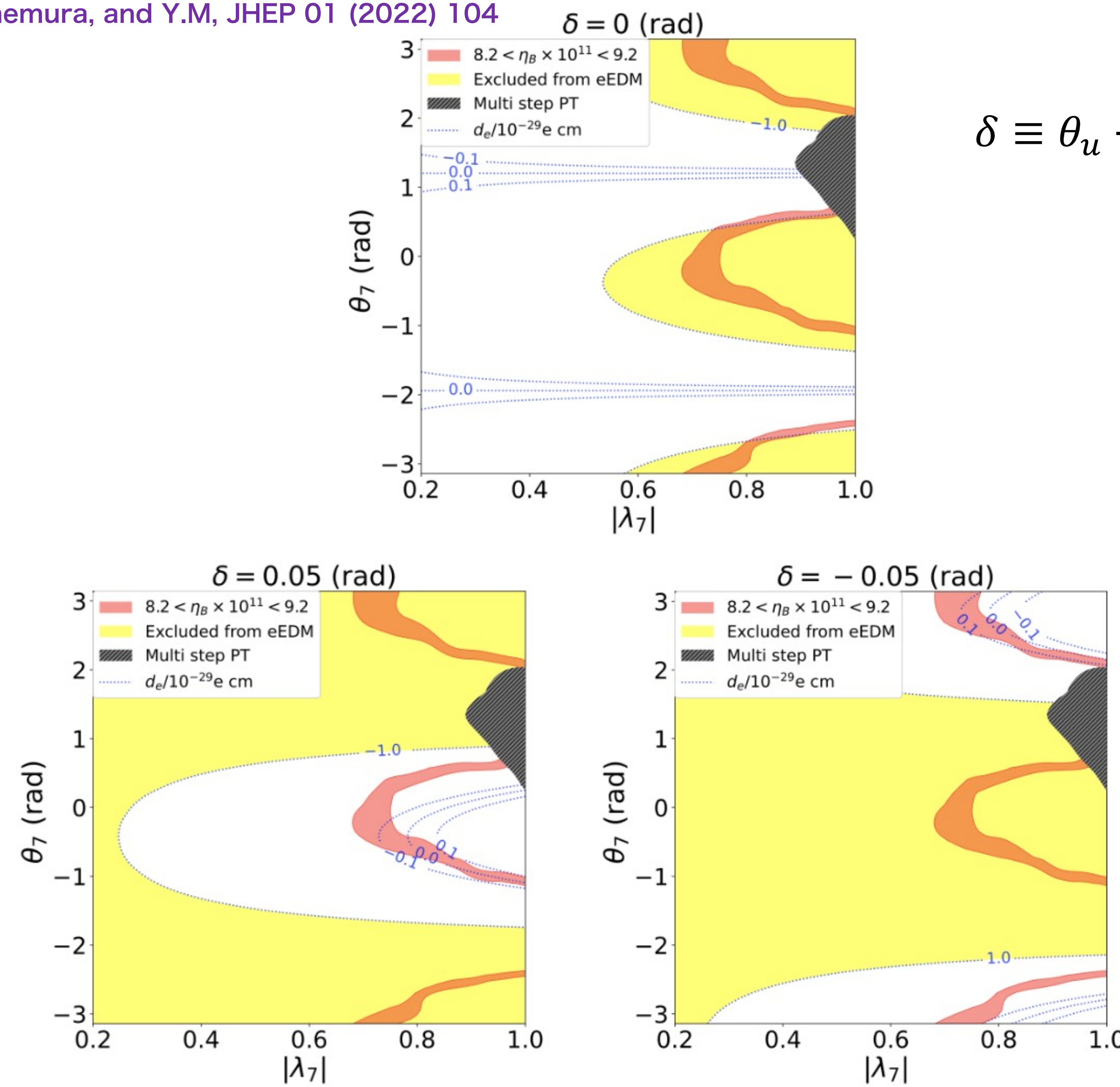

$$\delta \equiv \theta_u - \theta_e$$

Flavor constrarints

Model	ς_d	ς_u	ς_l
Type I	$\cot\beta$	$\cot\beta$	$\cot\beta$
Type II	$-\tan\beta$	$\cot\beta$	$-\tan\beta$
Type X	$\cot\beta$	$\cot\beta$	$-\tan\beta$
Type Y	$-\tan\beta$	$\cot\beta$	$\cot\beta$
Inert	0	0	0

Haller *et al.* Eur. Phys. J. C 78 (2018);

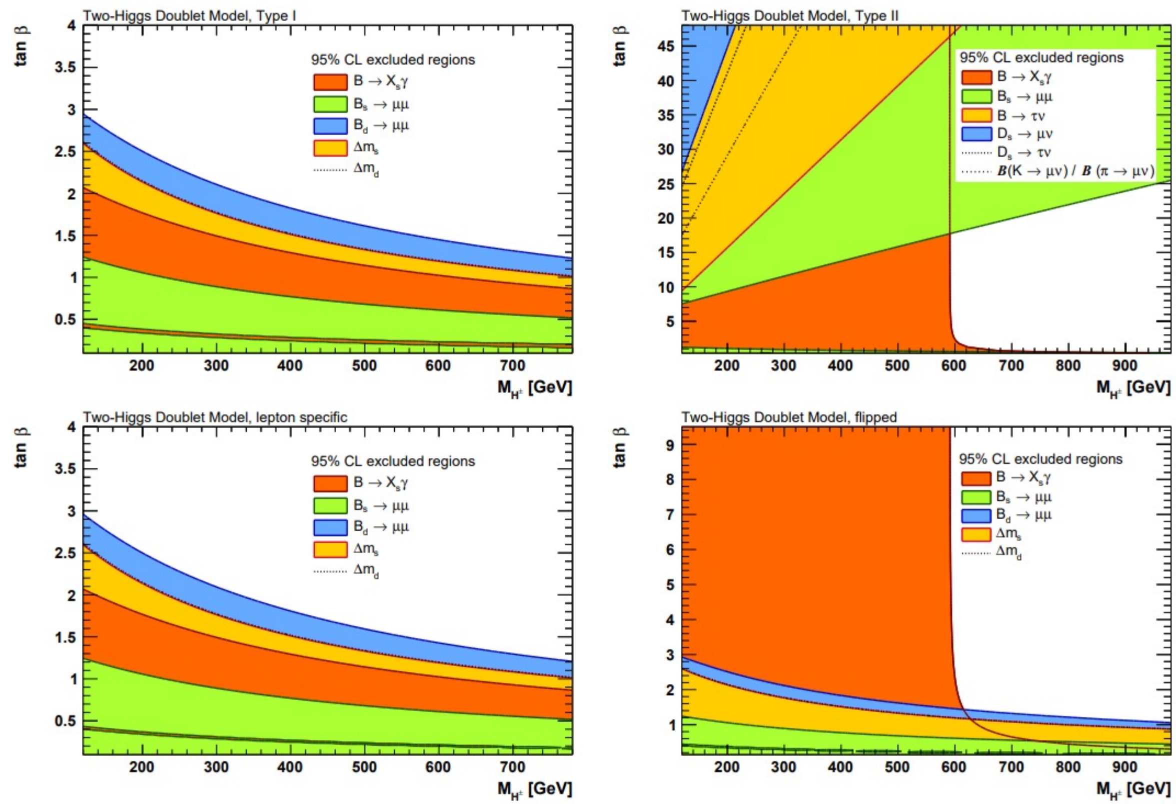

Type Ⅰ like

$$|\zeta_u| = |\zeta_d| = |\zeta_e| = \cot\beta$$

Type X like

$$|\zeta_u| = |\zeta_d| = \cot\beta$$

$$|\zeta_e| = -\tan\beta$$

$$m_{H^\pm} \simeq 300\text{GeV}, |\zeta_u| \lesssim 0.4$$

Collider constraints

Aiko, Kanemura, Kikuchi, Mawatari, Sakurai and Yagyu, Nucl. Phys. B 966 (2020)

Model	ς_d	ς_u	ς_l
Type I	$\cot\beta$	$\cot\beta$	$\cot\beta$
Type II	$-\tan\beta$	$\cot\beta$	$-\tan\beta$
Type X	$\cot\beta$	$\cot\beta$	$-\tan\beta$
Type Y	$-\tan\beta$	$\cot\beta$	$\cot\beta$
Inert	0	0	0

Current

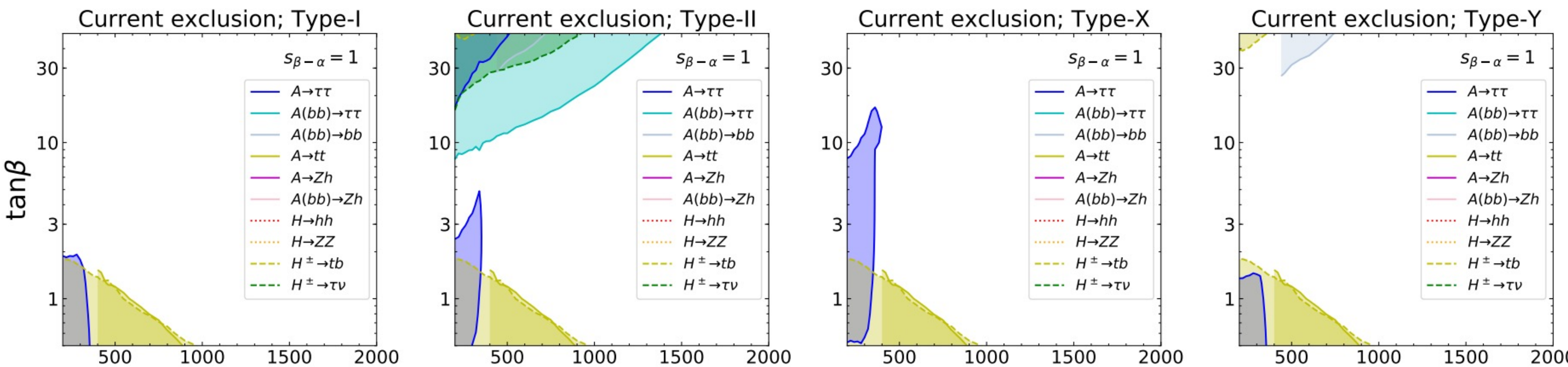

$$H_{2,3} \to \tau\tau$$
$$H_{2,3} \to tt$$
$$H^{\pm} \to tb$$

HL-LHC

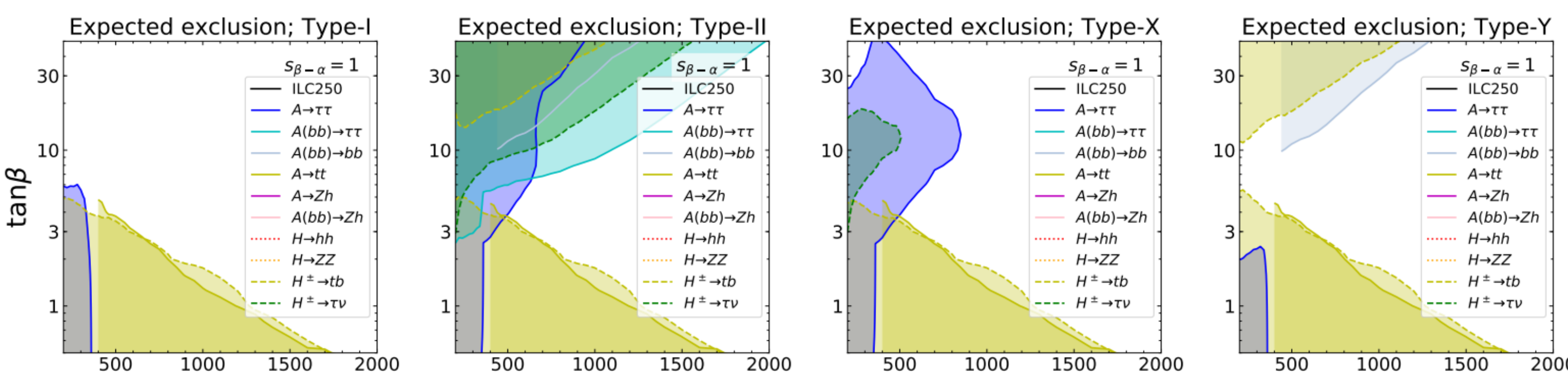

Other EDMs

Current
$|d_e| < 1.1\times10^{-29}$ (ThO)
$|d_\mu| < 1.5\times10^{-19}$(g-2)
$|d_\tau| < O(10^{-17})$ (Belle)
$|d_\tau| < 1.6\times10^{-18}$(from eEDM)

Expected
$|d_e| < O(10^{-30})$
$|d_\mu| < O(10^{-21})$
$|d_\tau| < O(10^{-18})$(Belle II)

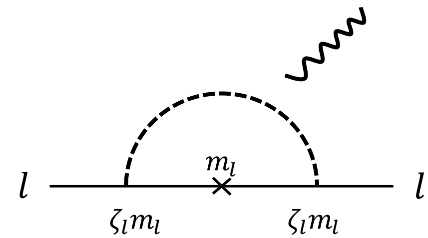

Theory
$d_e(1loop) = O(10^{-34})$ $\kappa = O(1)$, 1 loop contributions are proportional to m_e^3.
$d_\mu(1loop) = O(10^{-27})$ $m_\mu \sim 200m_e$
$d_\tau(1loop) = O(10^{-24})$ $m_\tau \sim 3600m_e$

$d_e(BZ) = O(10^{-28})$ $|\zeta| = O(10^{-1})$, BZ contributions are proportional to m_e
$d_\mu(BZ) = O(10^{-26})$ $m_\mu \sim 200m_e$
$d_\tau(BZ) = O(10^{-25})$ $m_\tau \sim 3600m_e$

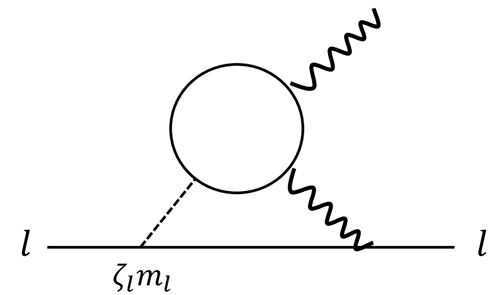

1 loop contributions include ζ^2 $\rightarrow$ with no lepton universality, $|\zeta_\tau|, |\zeta_\mu| \gtrsim O(10^3)$ are excluded.

Electroweak baryogenesis

EWPT is occurred at the temperature T_n,

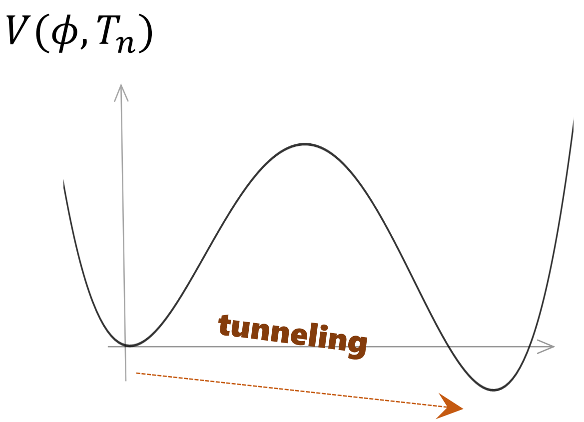

T_n determined by the condition

(The possibility of tunneling per Hubble) $\sim \mathcal{O}(1)$.

Sphaleron process ($\Delta B \neq 0$) frequently occurs in symmetric phase.

Left-handed baryons outside the wall are converted into baryon number.

Sphaleron process decouple in broken phase.
(Baryon number is conserved)

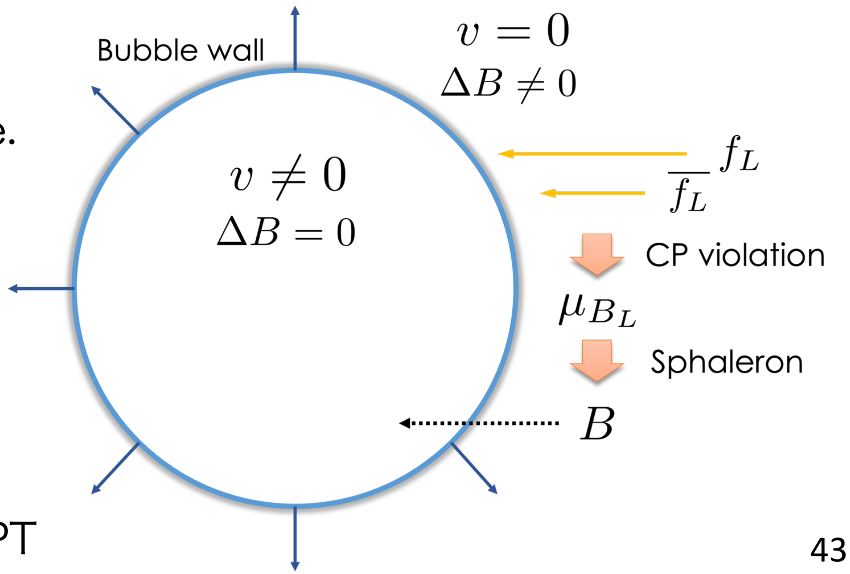

Sphaleron decoupling condition

$$\Gamma_{sph}^{brk}(T_n) < H(T_n) \implies \frac{v_n}{T_n} \gtrsim 1$$

→ "Strongly" first order PT